Palaeogeography, Palaeoclimatology, Palaeoecology 616 (2023) 111476

Contents lists available at ScienceDirect

Palaeogeography, Palaeoclimatology, Palaeoecology

journal homepage: www.elsevier.com/locate/palaeo

Mammalian turnover as an indicator of climatic and anthropogenic landscape modification: A new Meghalayan record (Late Holocene) in northern Iberia

Adrián Álvarez-Vena [a,*], Ana B. Marín-Arroyo [b], Diego J. Álvarez-Lao [a], César Laplana [c], Martín Arriolabengoa [d], Daniel Ballesteros [e], Arantza Aranburu [d], Peru Bilbao [d], Ángel Astorqui [f], Yolanda Díaz-Casado [f]

[a] Department of Geology, University of Oviedo, C/ Jesús Arias de Velasco s/n, 33005 Oviedo, Spain
[b] EvoAdapta Group, Universidad de Cantabria, 39005 Santander, Spain
[c] Museo Arqueológico y Paleontológico de la Comunidad de Madrid, Pza. Bernardas s/n, 28801, Alcalá de Henares, Madrid, Spain
[d] Department of Mineralogy and Petrology, University of the Basque Country, UPV/EHU, Leioa, Spain
[e] Department of Geodynamics, University of Granada, Campus de Fuentenueva s/n, Granada, Spain
[f] Tanea Documentación y Conservación SL, C/ Juan José Pérez del Molino 16, 39006 Santander, Spain

ARTICLE INFO

Editor: Dr. Howard Falcon-Lang

Keywords:
Climatic change
Chalcolithic
Bronze Age
Iron Age
Micromys minutus
Mus musculus

ABSTRACT

The Punta Lucero III cave is a natural trap where abundant vertebrate remains were accumulated during the Meghalayan (Late Holocene). To better understand the paleoenvironmental conditions in which this record was accumulated, the micromammal assemblage, comprising a minimum number of 1396 individuals belonging to 19 taxa, was studied using the Mutual Ecogeographic Range and the Habitat Weighting Method. Throughout ~2600 years, the micromammal community's quick turnover reflected a shift from patchy forests and humid meadows to open, shrubbier grasslands. The Late Holocene Thermal Maximum's humid and mild climatic conditions underwent a cooling and aridification phase, coeval with the Iron Age Cold Epoch. These concluded in a slight temperature rising, coeval with the Roman Warm Period. Macromammals experienced a shift from wild populations to domestic herds. Therefore, this work discusses a broader context for this mammalian turnover from a human cultural perspective.

1. Introduction

The Holocene was considered a relatively warm and stable epoch compared to the last glacial period (Dansgaard et al., 1993). Nevertheless, abrupt climatic changes and cooling events identified throughout the Holocene (Alley et al., 1997; Bond et al., 1997; Mayewski et al., 2004; Walker et al., 2018), even if weaker than those of the Last Glacial Cycle, have been intense enough to cause the rise and collapse of significant cultures and civilisations worldwide (Van Geel et al., 1996; deMenocal, 2001; Büntgen et al., 2011).

Principal warming or cooling trends at millennial timescales are caused by orbital forcing (deMenocal et al., 2000; Mayewski et al., 2004; Wanner et al., 2008) in addition to fluctuations in total solar irradiance and peaks of volcanic activity, which are also related to abrupt climate shifts (Bray, 1971; Van Geel et al., 1996; Bond et al., 2001; Mayewski et al., 2004; Wanner et al., 2008; Steinhilber et al., 2009; Miller et al., 2012; Sigl et al., 2015; Borzenkova et al., 2015). However, since the end of the Pleistocene and, especially during the Holocene, human activity has become an increasing force shaping the terrestrial and marine ecosystems (Vitousek et al., 1997; Crutzen, 2002; Doughty et al., 2010; Ellis, 2011; Barnosky, 2008, 2013; Boivin et al., 2016), causing a chemical fingerprint, both on a regional and global scale (Ruddiman and Thomson, 2001). From Mid-Holocene onwards, human activities such as animal husbandry, agriculture, and metallurgy, have had a significant impact on the landscapes of the regions inhabited by humans, including the Iberian Peninsula, making anthropogenic and climatic signals often indistinguishable in pollen records (Carrión et al., 2010). Due to this climatic and anthropogenic influence, mammals have experienced significant range shifts, extinction events, extirpations, and domestication processes (Rosengren et al., 2021). In this sense, the Holocene warming

* Corresponding author.
E-mail address: adrianalvarezvena@geol.uniovi.es (A. Álvarez-Vena).

https://doi.org/10.1016/j.palaeo.2023.111476
Received 15 January 2023; Received in revised form 23 February 2023; Accepted 24 February 2023
Available online 1 March 2023

and the development of human cultures also led to the turnover of the Iberian mammal communities. While domestic herds progressively replaced wild macromammals, micromammal assemblages, whose geographical distribution was affected by habitat changes (climatic or human-driven), also reflected the arrival of allochthonous commensal species (Altuna, 1980; Cuenca-Bescós et al., 2009; López-García et al., 2013; Bañuls-Cardona et al., 2017a; Domínguez García et al., 2019; Domínguez García et al., 2020; Domínguez-García et al., 2022; Moclán et al., 2023). For this reason, macro- and, particularly, micromammals are a valuable source of paleoenvironmental information that has been successfully analysed from diverse perspectives at key sites of the Cantabrian Region (e.g., Altuna, 1980; López-García, 2008; Cuenca-Bescós et al., 2009, 2012; Álvarez-Lao, 2014; Ballesteros et al., 2020; Álvarez-Vena et al., 2021; Jones et al., 2019, 2021).

Iberian macromammal assemblages from Holocene sites are mainly associated with archaeological contexts (Altuna, 1980; Mariezkurrena, 1990; Castaños, 1997; Altuna and Mariezkurrena, 2012; Vega-Maeso et al., 2016). Consequently, they are biased by anthropogenic activity. On the other hand, micromammal accumulations usually result from the predatory activity of raptors or mammalian carnivores (Andrews, 1990; García-Morato et al., 2023). Although these remains can be found in assemblages that do not necessarily involve predation (as in the case of natural traps, e.g., Álvarez-Lao et al., 2020), these kinds of sites are scarce in the literature. In our study case, accidental falling and nocturnal birds of prey are the most likely accumulating agents of the micromammals' assemblage. Still, according to the generalist habits of owls, they accurately represent the environment in which they hunt (Andrews, 1990). In this context, the site presented here is of great relevance as it yielded a Holocene mammal association mainly formed in a natural pitfall trap (at least in the case of macromammals), i.e., without bias by humans or specialised predators, offering an exceptional opportunity to understand the climatic change and human-environment interactions during the Meghalayan (Late Holocene) at the Cantabrian Region.

2. The Punta Lucero III site

2.1. Geographic context

The Punta Lucero III site (PL-III) is located at the eastern end of the Cantabrian Region, a strip of land (30–50 km wide) with rugged relief that extends along the north of the Iberian Peninsula. It is a karst shaft (vertical cave) situated on the northern slope of the Punta Lucero mount (43°21′34.44"N, 3°6′10.31"W, 240 m asl; Fig. 1) in the municipality of Zierbena/Ciervana (Bizkaia, Basque Country, northern Spain). This mountain flanks the west bank of the Nervión River mouth, where the Bilbao Port has been built (Fig. 1C-D). The site formed within the Lower Cretaceous limestone (calcarenite), sandstone and shale (Garrote et al., 1993) and forms part of a karst coastal area developed in a vadose environment during the Quaternary (Aranburu et al., 2015). Currently, the cave is located at the highest point of a quarry, whose exploitation began during the construction of the Bilbao seaport. However, before these works, it was located halfway up the slope, between the top of the mount and the Cantabrian Sea (Fig. 1E). Nowadays, this territory is part of the Euro-Siberian biogeographic region. The site is in the Atlantic climatic domain, characterised by temperate summers, mild winters, and no dry season (type Cfb according to the Köppen-Geiger classification; Beck et al., 2018). The mean annual temperature (MAT) at Zierbena is 13.9 °C, with maximum and minimum month-mean temperatures of 19.8 and 8.7 °C, respectively. Precipitation is distributed throughout the year, reaching an annual mean of ~1150 mm (Couto et al., 2011). However, the plant communities in this area have 30% of Mediterranean species (Patino et al., 2002). Some of these taxa expanded due to human activities such as the repeated use of fire to obtain pasture, as is the case of the holm oak (*Quercus ilex*) and the Kermes oak (*Quercus coccifera*), adapted to live in more extreme conditions than the Atlantic species (Patino et al., 2002).

Direct evidence of the human presence in Punta Lucero dates to times even before the formation of the studied sequence, as evidenced by the human remains (*Homo sapiens* bones) found at mount ridge by Gómez-Olivencia et al. (2015) in the sites of Punta Lucero II (5566–5318 cal yr BP) and Covachón III (4796–4424 cal yr BP), at ~200 and ~ 500 m from the PL-III shaft respectively. In the nearby site of Pico Ramos, it has also been found a sepulchral context of Chalcolithic age (5862–4295 cal yr BP) containing human skeletal remains of a minimum of 104 individuals (Baraybar and de la Rúa, 1995; Zapata, 1995). The palynological study of Pico Ramos Chalcolithic burials depicted an open landscape with signals of anthropisation, in which a mixed-oak grove formation of temperate and humid character was developed (Iriarte, 1994).

2.2. Stratigraphy

Before the quarry exploitation, the studied sequence consisted of a cave infill (Fig. 2) whose entrance was above the current level. The homogeneous sedimentary fill, mainly consisting of large limestone clasts and loamy sediment, was sampled at different depth intervals from its top towards its base, sometimes coinciding with stratigraphic levels of contrasting characteristics and, on others, within more thick and homogeneous sets. Due to the narrow excavation area, it was impossible to preserve a stratigraphic profile, so we divided the sequence into different stratigraphic sections each time we extracted a group of large limestone blocks so that bone samples could be grouped. Sections or levels were labelled F to A, from bottom to top of the preserved sequence. The depth was measured from the top of the remnant deposit, partially exposed after the last blasting works in the quarry. To identify differences in the sedimentary sequence, petrographic and mineralogical analyses were made in stratigraphic levels F, D, and C. Overall, they disclose matrix-supported microfacies, with fine to medium sub-angular quartz grains, mainly of sedimentary rocks but also few chert and metamorphic quartz (Appendix 1). Level F is at the bottom of the sequence, lying over the unexcavated deposit. This level was established by its high microcharcoal content in greyish sediment. Level F was under a big limestone block; sediment containing this block was named Level E. Level D was determined after finding the first cervid remains. Level C was labelled after the excavation of Level B, which was an unstable infill. Samples collected during the surface cleaning and the removal of isolated bones before the excavation of Level B were grouped in Level A since most of them fell from the lateral or above. Therefore, Level A must be considered with caution as a reworked sample.

3. Materials and methods

The mammal remains studied in this work come from the rescue excavations in the Punta Lucero quarry (Fig. 1D; Fig. 2) in September 2019. The stabilisation blasting at the quarry was supposed to destroy the cave. However, this did not happen, so the remaining stratigraphic sequence is still preserved at the site.

3.1. Stratigraphic study

The stratigraphic section of the PL-III site was divided into levels based on the nature, colour, granulometry, cohesivity, sedimentary structures, and relative abundance of paleontological remains (e.g., Arriolabengoa et al., 2015). The top of the PL-III site was destroyed by quarrying; thus, level depth was measured considering the excavation surface in September 2019. The stratigraphic section was complemented by microscopical observations of unconsolidated sediments and X-Ray Diffraction (XRD) analysis to characterise mineralogy and microfacies and to infer the sediment provenance. See Appendix 1 for further details.

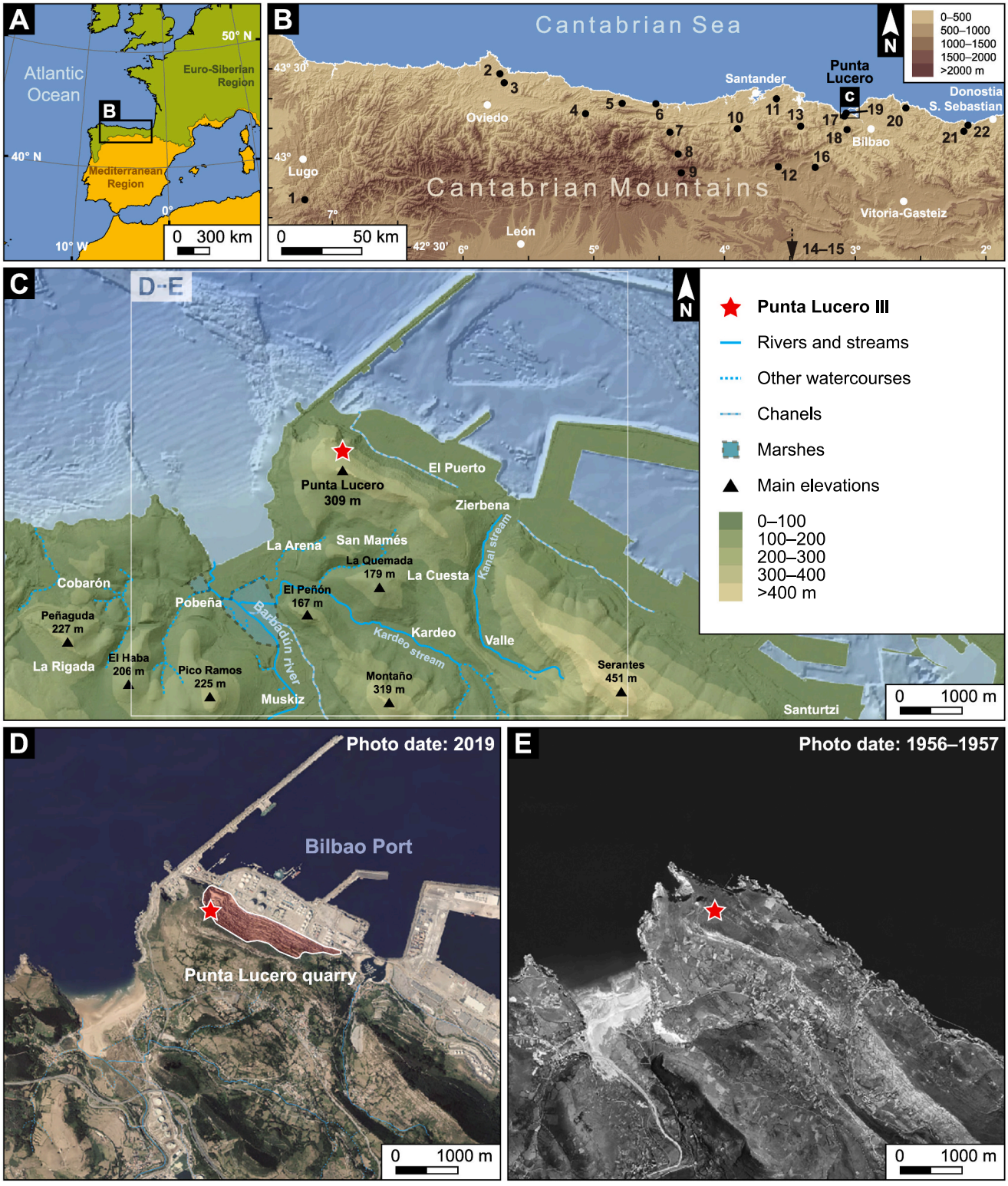

Fig. 1. Geographical context for the Punta Lucero III site. (A) Location of the Cantabrian Region (B) in the Iberian Peninsula. (B) Other sites mentioned in this work: 1 Valdavara-1; 2 Monte Areo mire; 3 El Olivo; 4 La Güelga; 5 Torca del León; 6 El Espinoso; 7 El Sertal; 8 Cueto la Avellanosa; 9 Cueva del Cobre; 10 La Molina peatbog; 11 La Garma; 12 Kaite; 13 El Mirón; 14 Cueva Mayor; 15 Mirador; 16 Zalama peatbog; 17 Pico Ramos; 18 Arenaza; 19 Punta Lucero-II and Covachón-III; 20 Kobaederra; 21 Amalda; 22 Herriko Barra. (C) Hypsometric background with 100 m altitude intervals of the Punta Lucero surroundings. (D–E) Orthophotography of the Punta Lucero surroundings: (D) after the stabilisation works in the quarry that allowed the discovery of the Punta Lucero shaft, and (E) before the construction of the Bilbao Port. Cartography and orthophotography from the geoEuskadi online GIS-viewer (Eusko Jaurlaritza/Gobierno Vasco).

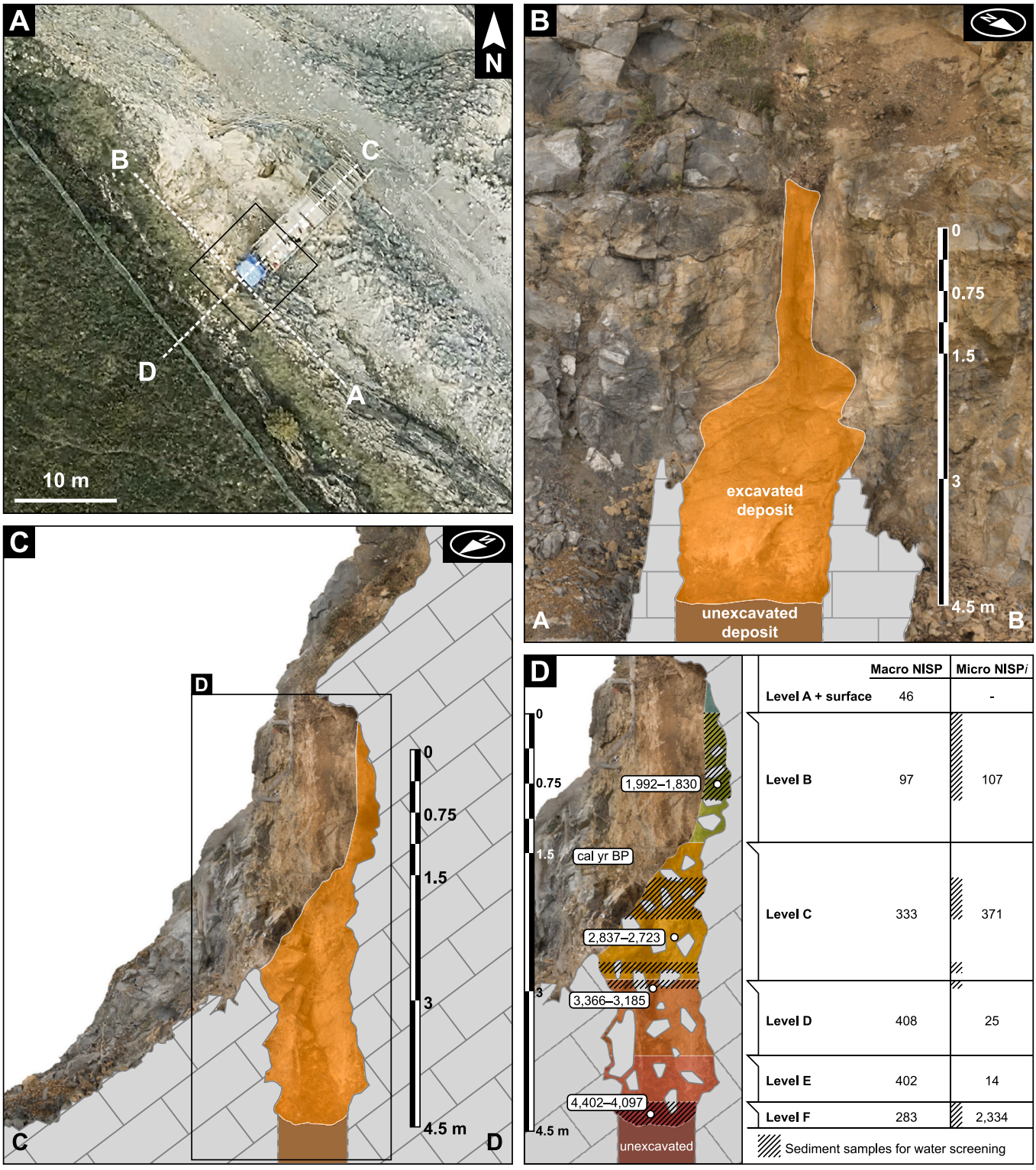

Fig. 2. Characterisation of the Punta Lucero III excavation. (A) Orthophoto of the excavation area. The projection of the sections in b and c is indicated. (B) A–B cross-section of the shaft. (C) C–D cross-section of the shaft. (D) Stratigraphic profile of the shaft infill. Small mammal NISP*i* omits the *Lepus* remains. Photogrammetric reconstructions of backgrounds from sections of B–D provided by GIM-Geomatics.

3.2. Dating

Three bone samples and two charcoals were selected for AMS radiocarbon dating and sent to the Beta Analytic laboratory (Miami, USA). Obtained ages and published dates discussed in this work were calibrated through the IntCal20 database (Reimer et al., 2020) in OxCal v.4.4.4 (Bronk Ramsey, 2009), considering the 2σ standard deviation (95.4% probability).

3.3. Collecting and sorting

3.3.1. Micromammals

A total of 24 samples of sediment (~10 kg each) were collected and water-screened using two superimposed sieves of 0.5 and 2 mm. The materials in the fine fraction (0.5–2 mm) were sorted by checking the samples with a binocular microscope under 10× magnification. The obtained bone remains were then classified and studied at the Geology Department of the University of Oviedo (Spain).

Taxonomic identifications were carried out employing a stereomicroscope Nikon SMZ800N, equipped with a 16 Mpx digital camera. Measurements were taken on the microscope photographs using Adobe Photoshop CC software. Due to their diagnostic value and potential of preservation, the anatomical elements selected for taxonomic identifications were the following: p3 and postcranial skeleton for lagomorphs; isolated molars for murids; m1 for arvicolines (also considering the M3 for the *Terricola* subgenus, and the M1 and M2 for the species belonging to the *Microtus* (*Agricola*) *agrestis* group); mandibles and maxillae for soricids and erinaceids; and upper molars and humeri for talpids. A comparative collection of micromammal skeletal remains obtained from recent barn owl pellets was also used.

Hares were identified following Palacios and López Martínez (1980), Llorente (2010), and Pelletier (2018). The general identification of rodents and shrews followed Román (2019) and Nores (1989), respectively. Detailed taxonomical and morphological analyses were based on: Krapp and Niethammer (1982), Nadachowski (1984), and Luzi and López-García (2019) for *Microtus* (*Agricola*) ex gr. *agrestis* (which includes the species *Mi.* (*Ag.*) *lavernedii*, *Mi.* (*Ag.*) *rozianus* and *Mi.* (*Ag.*) *agrestis*) and *Microtus* (*Microtus*) *arvalis* lower dentition; Nores et al. (1982), Pemán (1983) and Barti (2006) for *Neomys* mandibles; Pasquier (1974), Nores (1988) and Knitlová and Horáček (2017) for *Apodemus* (*Sylvaemus*) dentition; Darviche et al. (2006) for *Mus*; and Niethammer (1990) and Gutiérrez et al. (2019) for *Talpa* humeri and upper molars respectively. The taxonomic classification followed the systematics proposed by Wilson et al. (2016, 2017) and Wilson and Mittermeier (2018), also considering the work of Kryštufek et al. (2020) for *Clethrionomys* and Kryštufek and Shenbrot (2022) for *Microtus* (*Terricola*) *pyrenaicus*. The number of specimens was obtained by counting the most frequent taxonomically identifiable element per species (NISP*i*, see Lyman, 1984). The relative abundance of each micromammal species was based on the minimum number of individuals (MNI), which was calculated considering the laterality of the most frequent diagnostic element.

3.3.2. Macromammals

The main macromammal remains from each level were recovered directly from the excavation surface and coordinated individually. In addition, sediment samples for mechanical sieving of the smaller bones and fragments were collected and labelled according to depth. Anatomical and taxonomical identifications followed the works of Pales and Lambert (1971), Schmid (1972), Barone (1976), and Hillson (2005). The Osteological Collection of the EvoAdapta group at the University of Cantabria was also used for comparison purposes.

The age at death has been estimated based on the molar development and the epiphyseal fusion degree of the limb bones. Age estimations followed the criteria published by Noddle (1974), Silver (1980), Mariezkurrena (1983), Azorit et al. (2002), and Tomé and Vigne (2003). Relative abundance is based on the number of identified specimens (NISP) with previous reassembling of the fragmented bones.

3.4. Preliminary identification of predatory alterations

To evaluate if the likely cause of the micromammal accumulation was other than the accidental falling to the cave, the enamel of arvicoline molars was analysed in search of alterations caused by digestion (and, consequently, predation), following Andrews (1990) and Fernández-Jalvo et al. (2016). The observed digestion signals were counted and classified according to the following categories: absent, light, moderate, heavy, and extreme (Andrews, 1990; Fernández-Jalvo et al., 2016). Macromammal bones were also observed using a Leica stereomicroscope at 10–80× magnification in search of predatory or natural alterations following Binford (1981) and Marín-Arroyo (2010).

3.5. Paleoenvironment

The landscape surrounding the PL-III shaft was inferred using the Habitat Weighting Method (HWM; Evans et al., 1981; Andrews, 2006; Blain et al., 2008; Cuenca-Bescós et al., 2009; López-García et al., 2014), which is based on the habitat-type preferences of each micromammal taxon. The obtained habitat types are the following: open dry (OD) comprises meadows under seasonal climate change, dry grasslands, and scrublands; open humid (OH) corresponds to evergreen meadows with dense pastures and suitable topsoil; open woodland (OW) represents woodland margins and forest patches with moderate ground cover; woodland (Wo) indicates mature forest; and water (Wa) corresponds to areas along freshwater streams, lakes, and ponds. The environmental preferences of each species were obtained from Nores (1989), Wilson et al. (2016, 2017), and Wilson and Mittermeier (2018). Hare (*Lepus europaeus*) remains were obtained simultaneously by excavation (throughout the complete sequence) and sieving. This makes them overrepresented in the sampling compared to the other micromammal species, which were only sampled in specific sections, so they have been excluded from landscape reconstructions. The house mouse (*Mus musculus*) is a commensal species of humans that commonly inhabits anthropic environments; therefore, it has not been included in the HWM calculations.

3.6. Paleoclimate

The climatic conditions at the time of each level's accumulation were estimated using the Mutual Ecogeographic Range (MER) method, based on microvertebrate associations (e.g., Martínez-Solano and Sanchiz, 2005; Blain et al., 2009, 2016; Fagoaga et al., 2019). This method is frequently used to calculate the mean annual temperature (MAT), the mean temperature of the warmest month (MTW), the mean temperature of the coldest month (MTC), and the mean annual precipitation (MAP). In this work, we have also used this method to obtain monthly rainfall and temperature values to observe seasonal patterns. These parameters were calculated by getting the common geographical areas (represented in a net of 10 × 10 km UTM squares) of each micromammal species association (including hares) from the PL-III sequence. The climatic data of the shared UTM squares for each assemblage and the current climatic data from the PL-III site were obtained using the online application agroclimap.aemet.es of the Iberian Climate Atlas (Couto et al., 2011). The current distribution of each species was obtained from Palomo et al. (2007).

4. Results

4.1. Radiocarbon dating

Obtained dates ranged from 4402 to 836 cal yr BP (Table 1). Four samples yielded an age according to their stratigraphical position. In contrast, sample Beta-541,219, a charcoal collected at the bottom of the excavated deposit, was likely an outlier as it provided the youngest date of the set (1055–836 cal yr BP).

4.2. Predatory activity

Teeth with signs of digestion are scarce in the micromammals' sample (<1%), but in the few cases of digested molars, they reached heavy to extreme corrosion. According to the classification proposed by

Table 1
Radiocarbon dates from Punta Lucero.

Level	Depth (cm)	Material	Method	Lab Ref	^{14}C	Deviation	cal yr BP[a]
B	77	Bone	AMS	Beta-629,438	1980	30	1992–1830
C	242	Bone	AMS	Beta-541,215	2630	30	2837–2723
D	296	Charcoal	AMS	Beta-541,218	3070	30	3366–3185
F	430	Bone	AMS	Beta-541,217	3830	30	4402–4097
F	445	Charcoal	AMS	Beta-541,219	1040	30	1055–836

[a] Calibrated using the software OxCal v.4.4.4 (Bronk Ramsey, 2009) against the IntCal20 curve (Reimer et al., 2020). Further data is provided in Appendix 2.

Andrews (1990), this suggests that category-5 predators, mainly mammalian carnivores, ingested those few individuals. However, most of the specimens observed (99%) do not show predation features.

The macromammal sample does not show butchery or burning (cooking) features. The only predator signals in the PL-III bone accumulation are those produced by carnivores (Table 5), affecting 6.2% of the specimens. Carnivore tooth marks are more common at levels C (12.3%) and B (9%), being scarcer at levels E (5.9%), F (5.3%), and D (4.6%).

4.3. Micromammal record

The Micromammal assemblage of the PL-III sequence yielded a minimum (MNI) of 1396 individuals belonging to 19 taxa (Table 2; Figs. 3–6; Appendix 3). Among rodents, arvicolines (Fig. 3; Table S3.1) are represented by genera *Arvicola* (*Ar. sapidus*), *Microtus* (*Mi.* (*Agricola*) *lavernedii*, *Mi.* (*Microtus*) *arvalis, Mi.* (*Terricola*) sp., *Mi.* (*Terricola*) *pyrenaicus*, and *Mi.* (*Terricola*) ex gr. *lusitanicus–duodecimcostatus*), and *Clethrionomys* (*Cl. glareolus*); additionally, murids (Fig. 4a–c) include three species belonging to three genera: *Micromys minutus* (Fig. 5A; Table S3.2), *Mus musculus*, and *Apodemus* (*Sylvaemus*) *sylvaticus* (Fig. S3.1; Table S3.3). In the eulipotyphlans order, the soricids family (Fig. 4d–i') yielded six taxa belonging to genera *Crocidura* (*Cr. russula* and *Cr. gueldenstaedtii*: Fig. S3.2; Table S3.4), *Sorex* (*Socoronatus* and *So. minutus*) and *Neomys* (*N. anomalus* and *N. fodiens niethammeri*: Fig. 5B; Table S3.5); talpids and erinaceids are represented by one species each: *Talpa aquitania* (Fig. S3.3; Fig. S3.4; Table S3.6) and *Erinaceus europaeus* respectively. Lastly, the morphology and size of the postcranial skeleton (Fig. 5C; Fig. S3.5a–d'; Table S3.7) and the lower third premolars (Fig. S3.5b) allowed us to assign the lagomorph remains to the species *Lepus europaeus*. Arvicolines yielded the most significant number of individuals from levels F, D, and B (Table 2; Fig. 6), being *Mi.* (*Ag.*) *lavernedii* the best-represented species at these levels (35.6–42.9%). Conversely, the lowest proportion of this arvicoline, reached at Level C (19.4–7.8%), matches a considerable increase in the abundance of *Cr. russula*, a soricid that is scarcely represented at the bottom of the sequence (levels F and D: 0.8% and 0% respectively).

We identified two types of micromammal associations in the PL-III sequence according to their shared distribution range (Appendix 4; Fig. 7). The first one, coming from Level F, cohabits nowadays in areas at the northern slope of the Cantabrian mountains (Fig. 7A), where oceanic influence is higher. Conversely, species associations from levels C and B, at present, mainly coexist at the southern slope of the Cantabrian mountains (Fig. 7B–C) in areas of a more continental climate.

4.4. Macromammal record

The studied sample comprises 3220 remains (NSP), of which 1569 (48.7%) could be taxonomically classified (Table 3). Among domestic ungulates, bovids dominate the assemblage (Fig. 8a–f), mainly sheep and goats (*Ovis orientalis aries*: Fig. 8a–a'; and *Capra aegagrus hircus*: Fig. 8b–d) at the top section of the stratigraphic sequence (levels C–B: Fig. 9; Table 3), followed by cattle (*Bos primigenius taurus*; Fig. 8e–f). Conversely, equids (*Equus* sp.) are barely represented, although these have yielded remarkably well-preserved remains (Fig. 8i). All the suid remains correspond to infantile (mostly) or young individuals (Fig. 8j–k): dentitions still retain the deciduous teeth in wearing (M3/m3 are not yet erupted at any of the individuals), and limb bones are not yet fully grown (epiphyses were not fused at the time of death). Consequently, it was not possible to ascribe these remains to the domestic pig or the wild boar, so they are classified as *Sus scrofa* ssp. Wild ungulates comprise two cervid species: the red deer (*Cervus elaphus*: Fig. 8g) and the roe deer (*Capreolus capreolus*: Fig. 8h–h'); both, especially the red deer, are well represented at the lower section of the sequence (levels F–D: Fig. 9; Table 3). Finally, most carnivore remains belong to the European badger (*Meles meles*). However, remains of canids have also been found, which, due to their small size, are ascribed to dogs (*Canis lupus familiaris*). The age profile of the assemblage (Table 4) is dominated by infantile (55.8%) and juvenile (24.4%) individuals, while adults (19.8%) are the less abundant group. In the case of *Equus* sp., *Cervus elaphus* and *Sus scrofa* ssp. samples, these reach 80% of infantile individuals.

4.5. Paleoenvironment

The different micromammal assemblages found at each of the studied layers of the PL-III sequence describe an open landscape in an evolving context (Table 6, Fig. 10D). Highest proportion of moisture indicators (OH: 47.9%) is at the bottom of the sequence (Level F), where lowest values of aridity were also obtained (OD: 0.6%). The mature forest signal is weak in most of the levels (Wo: <1%), reaching the highest values also at Level F (Wo: 2.4%). However, aridity indicators increase towards de top of the deposit, especially at Level C (OD: 42.5–52.9%). Regarding the micromammal sample from Level D, this is not quantitatively enough (MNI: 14) to make reliable interpretations, though, except for the higher proportion of aquatic indicators (ΔWa: +20%) and the slightly increasing aridity in this level (ΔOD: +4.7%), a certain similarity among levels D and F samples can be observed. The open landscape inferred from micromammal assemblage is consistent with the stratigraphic study of the PL-III site (Appendix 1). This study suggests sediments resulting from soil erosion and run-off processes in the surroundings of the paleontological site. Both processes are common in an open landscape with little vegetation to protect the soil from erosion and improve water infiltration rather than runoff processes (García-Ruiz, 2010).

4.6. Paleoclimate

According to MER results (Appendix 4; Fig. 11; Fig. 12A), mean temperatures during the formation of Level F (MAT: 12.5 ± 0.7 °C), which are slightly under the present-day data (MAT: 13.9 ± 0.2 °C), are decreasing towards levels C (MAT: 9.9 ± 1.7 °C) and B (MAT: 10.3 ± 1.3 °C), especially the winter temperatures (Figs. 13–14a). The mean rainfall of Level F (MAP: 1359 ± 298 mm) is slightly over current mean values (MAP: 1156 ± 17 mm), though it also decreases in levels C (MAP: 968 ± 319 mm) and B (MAP: 893 ± 339 mm).

Monthly temperature and rainfall estimations (Appendix 4; Fig. 11) obtained for Level F display the typical Atlantic pattern of the Cantabrian coast. However, the climographs of levels C and B show an increasing continental trend, with more extreme differences between

Table 2
Micromammal species from Punta Lucero and their weighted habitat-preferences.

	Level F (Sample z: 445–420)			Level D (Sample z: 296–288)			Level C-bottom (Sample z: 280–269)			Level C-middle (Sample z: 222–208)			Level C-upper (Sample z: 208–177)			Level B (Sample z: 0–93)			Habitat type				
	$NISP_i$	MNI	%MNI	$NISP_i$	MNI	%MNI	$NISP_i$	MNI	%MNI	$NISP_i$	MNI	%MNI	$NISP_i$	MNI	%MNI	$NISP_i$	MNI	%MNI	Wa	OD	OH	OW	Wo
Arvicola sapidus	6	4	0.4	4	3	21.4										2	1	1.7	1				
Microtus (Agricola) lavernedii	746	389	35.6	8	6	42.9	41	21	18.6	6	4	7.8	11	7	19.4	47	24	40.0			0.5	0.5	
Microtus (Microtus) arvalis				1	1	7.1	11	6	5.3	2	1	2.0	1	1	2.8	13	7	11.7		0.75		0.25	
Microtus (Terricola) sp.	266	21	1.9	1	1	7.1	4	2	1.8	1	1	2.0									0.5	0.5	
Mi. (Te.) ex gr. *lusitanicus-duodecimcostatus*	176	88	8.1													1	1	1.7			0.5	0.5	
Mi. (Te.) pyrenaicus	57	32	2.9																		0.5	0.5	
Clethrionomys glareolus	16	11	1.0				2	1	0.9														1
Mus musculus	2	1	–							2	1	–							–	–	–	–	–
Apodemus (Sylvaemus) sylvaticus	315	161	14.7	2	2	14.3	17	10	8.8	7	4	7.8	1	1	2.8	5	4	6.7				1	
Micromys minutus	10	7	0.6																		1		
Sorex minutus	35	20	1.8																		0.25		0.75
Sorex coronatus	532	274	25.1				7	5	4.4	7	4	7.8	1	1	2.8	11	5	8.3			0.75	0.25	
Neomys fodiens niethammeri	32	16	1.5																0.75		0.25		
Neomys anomalus							2	2	1.8				1	1	2.8				0.25		0.75		
Crocidura russula	15	9	0.8				112	58	51.3	62	35	68.6	45	24	66.7	24	13	21.7		0.75		0.25	
Crocidura gueldenstaedtii	96	49	4.5																		0.5	0.5	
Talpa aquitania	20	10	0.9	1	1	7.1	10	8	7.1	3	2	3.9	1	1	2.8	5	4	6.7			0.75	0.25	
Erinaceus europaeus	1	1	0.1													1	1	1.7			0.25	0.25	0.5
Total	**2325**	**1093**	**100**	**17**	**14**		**206**	**113**		**90**	**52**		**61**	**36**		**103**	**60**						

winter and summer temperatures and a considerable decrease in rainfall throughout the year.

5. Discussion

5.1. Origin of the mammal assemblage

Predation signals observed in the micromammal sample only affect a few isolated molars (<1%), which reach a high–extreme degree of enamel corrosion produced by digestion. These specimens could get the deposit in the stomach of the trapped carnivores (*Canis lupus familiaris* or *Meles meles*) since no other features exclusively produced by predators were observed. The taphonomic signals caused by the intense rockfall or the excavation procedures could be masking those produced by nocturnal birds of prey or other predators, which cannot definitively be ruled out of acting as accumulating agents. In any case, no bias is observed regarding the prey type- or size range. Therefore, the most likely causes of the micromammal sample accumulation are accidental falling in the cave, pellet regurgitation by nocturnal birds of prey, or a combination of both. We do not exclude that run-off processes deposited some micromammal remains after small transport (<5–10 m) from the vicinity of the PL-III site (Appendix 1). Otherwise, the low transport was insufficient to round off the skeletal/dental remains.

Regarding the macromammal sample, the proportion of carnivore tooth marks (6.2%: Table 5) is significantly lower than that observed in badger dens by Arilla et al. (2020) and Mallye et al. (2008), whose samples showed this type of alteration in the 40% and the 20–30% of the bones, respectively. The mortality profile of the macromammal sample (Table 4) also displays clear differences with the obtained at badger burrows by Arilla et al. (2020), where the 64% of the individuals are adults, 28% are juvenile, and 8% are infantile. Conversely, this pattern inverses at PL-III (adult 15.9%; juvenile 23.8%; infantile 60.3%). Natural pitfall traps, such as the one studied by Álvarez-Lao (2014), also provided samples dominated by young individuals since those are more likely to get involved in potentially fatal situations. In this case, carcasses of dead animals trapped in the cave would have been scavenged by badgers (*Meles meles*), whose tooth marks are compatible with those observed in PL-III. Therefore, badgers, the best-represented carnivore in the assemblage, could have fallen into the cave while chasing the smell of the cadavers.

5.2. Paleoenvironment and paleoclimate

The micromammal accumulation of the PL-III sequence stands out by its great abundance, species richness, and state of preservation. Most of the identified species inhabit the region nowadays; however, when compared to a sampling on regurgitation pellets performed by González Oreja et al. (1993), some differences can be highlighted: modern assemblages in the cave surroundings (Fig. 6) include the brown rat (*Rattus norvegicus*) while lacking other taxa such as the bank vole (*Clethrionomys glareolus*) and the Güldenstädt's shrew (*Crocidura gueldenstaedtii*), which are displaced to less-anthropized inland areas (Palomo et al., 2007), or the common vole (*Mi.* (*Mi.*) *arvalis*), whose presence at north-western Iberia is today limited to the southern slope of the Cantabrian mountains.

Concerning the evolution of the PL-III micromammal association (Fig. 6), some taxonomic and biogeographical remarks of paleoenvironmental value can be addressed. Among rodents, species of the field vole group (*Microtus* (*Agricola*) ex gr. *agrestis*) are some of the most frequent micromammals in modern and fossil assemblages of the region. The phylogeny of this group has been under continuous revisions, leading to the recognition of three different species under similar morphological features (Paupério et al., 2012; Wilson et al., 2017). At the time of the formation of this paleontological site, the northern and southern lineages of the *Mi.* (*Ag.*) *agrestis* group (*Mi.* (*Ag.*) *lavernedii*, *Mi.* (*Ag.*) *rozianus* and *Mi.* (*Ag.*) *agrestis*) had already split since, according to

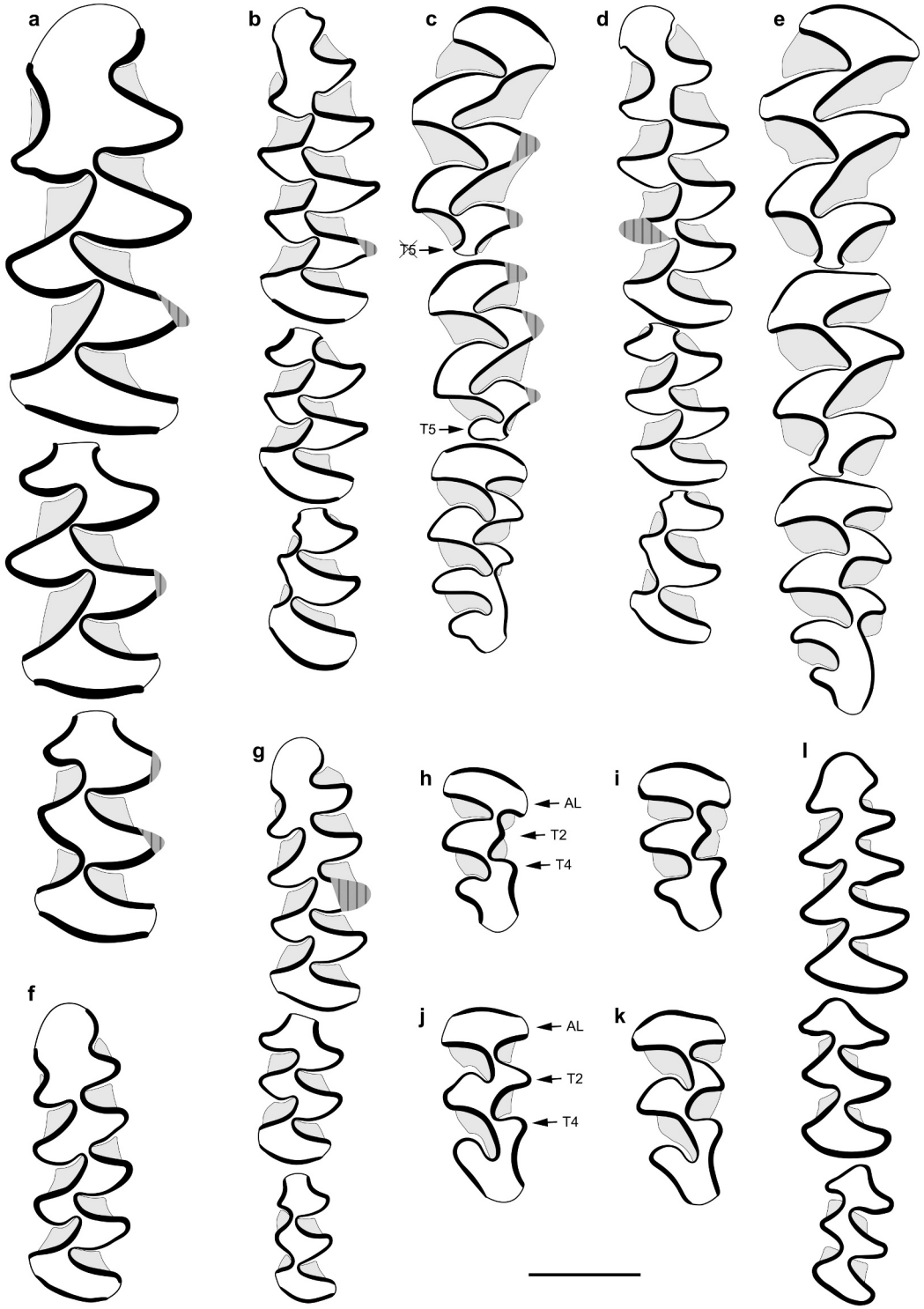

Fig. 3. Selected arvicoline specimens from Punta Lucero III. *Arvicola sapidus*: left m1–m3 from Level F in occlusal (a) view. *Microtus* (*Agricola*) *lavernedii*: left m1–m3 from Level F in occlusal (b) view and left M1–M3 from Level C in occlusal (c) view. *Microtus* (*Microtus*) *arvalis*: left m1–m3 from Level C in occlusal (d) view, and left M1–M3 from Level C in occlusal (e) view. *Microtus* (*Terricola*) sp.: left m1 from Level F in occlusal (f) view, and left m1–m3 from Level F in occlusal (g) view. *Microtus* (*Terricola*) ex gr. *lusitanicus–duodecimcostatus*: left M3 from Level F in occlusal (h) view and left M3 from Level F in occlusal (i) view. *Microtus* (*Terricola*) *pyrenaicus*: left M3 from Level F in occlusal (j) view and left M3 from Level F in occlusal (k) view. *Clethrionomys glareolus*: left m1–m3 from Level F in occlusal (l) view. AL: anterior loop. T: triangle. Scale bar 1 mm.

Paupério et al. (2012), they did at around the Last Glacial Maximum (LGM). The frequency of M1 with a postero-lingual triangle, like the one observed in the M2, is a discriminant feature among *Mi.* (*Ag.*) ex gr. *agrestis* species (Krapp and Niethammer, 1982; Wilson et al., 2017). The low proportion of M1 presenting this triangle (1.5%: Table S3.1) has allowed us to ascribe the field-vole specimens from PL-III to the Mediterranean field vole (*Mi.* (*Ag.*) *lavernedii*), which is the current representative of this group in the region. Nowadays, *Mi.* (*Ag.*) *lavernedii* spreads throughout the Cantabrian Region (Palomo et al., 2007). Conversely, *Microtus* (*Microtus*) *arvalis* (common vole), a species of more

Fig. 4. Selected murid, soricid, and talpid specimens from Punta Lucero III. *Micromys minutus*: left mandible from Level F with m1 in lingual (a) and occlusal (a') views. *Mus musculus*: Left maxilla fragment from Level F with M1–M2 in occlusal (b) view. *Apodemus* (*Sylvaemus*) *sylvaticus*: left M1–M3 series from Level F in occlusal (c) view. *Neomys fodiens niethammeri*: right mandible from Level F in posterior (d) and labial (d') views. *Neomys anomalus*: right mandible from Level C in posterior (e) and labial (e') views. *Sorex coronatus*: right mandible from Level F in posterior (f) and labial (f') views. *Sorex minutus*: right mandible from Level F in posterior (g) and labial (g') views. *Crocidura gueldenstaedtii*: right mandible from Level F in posterior (h) and labial (h') views. *Crocidura russula*: right mandible from Level C in posterior (i) and labial (i') views. *Talpa aquitania*: left humerus from Level C in posterior (j) view. Analogous anatomical elements have been flipped horizontally to show them from the same side for comparison purposes. Scale bars 1 mm.

continental requirements (Nores, 1989), lives south of the watershed, in the northern half of the Iberian Plateau (Nores, 1989; Palomo et al., 2007). Concerning proportion among these species, in Level C, a decrease in the abundance of *Mi.* (*Ag.*) *lavernedii* is observed along with the appearance of *Mi.* (*Mi.*) *arvalis*. However, *Mi.* (*Ag.*) *lavernedii* prevails at Level B, coinciding with the highest abundance ratio of *Mi.* (*Mi.*) *arvalis* in the sequence. It can also be seen that when *Mi.* (*Ag.*) *lavernedii* increases, also does *Arvicola sapidus*, a temperate-affinity water vole from southwestern Europe. This pattern, in which the initial absence of *Mi.* (*Mi.*) *arvalis* is followed by its increasing abundance, is also observed at La Güelga (Asturias, ~48–37 ka, Álvarez-Vena et al., 2021), an MIS 3 site in which an alternation of climatic changes from temperate to cold stadials was reported in a scenario of increasing aridity.

Regarding the remnant vole taxa from PL-III is also remarkable the occurrence of at least two species of the *Terricola* subgenus: *Mi.* (*Te.*) *pyrenaicus* (the Pyrenean pine vole) and *Mi.* (*Te.*) ex gr. *lusitanicus–duodecimcostatus*. Observed morphotypes of the M1 point to the presence of both Mediterranean (*Mi.* (*Te.*) *duodecimcostatus*) and Lusitanian (*Mi.* (*Te.*) *lusitanicus*) pine voles but overlapping morphological variability did not make us possible to discriminate between these species, which was even more difficult due to the co-occurrence of the Pyrenean pine vole. For this reason, the total MNI of the *Terricola* subgenus has been calculated based on the m1. However, the proportion of individuals of each species belonging to this subgenus has been

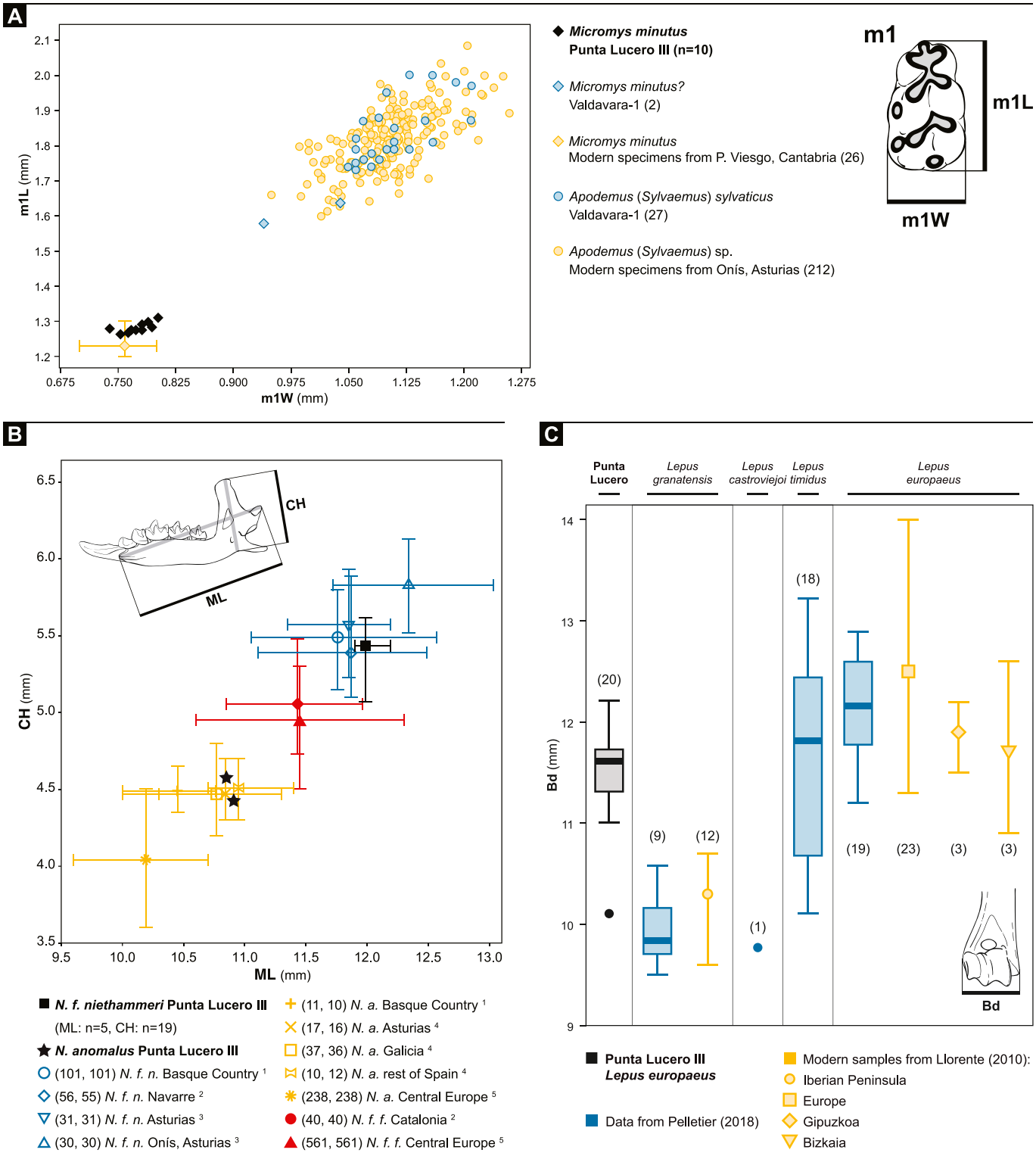

Fig. 5. Biometrical study of selected taxa. (A) Bivariate plot comparing the length (m1L) and the width (m1W) of the Punta Lucero III lower first molars of *Micromys minutus* with those of the oldest record of the species at the Iberian Peninsula (Valdavara-1: López-García et al., 2011). Modern *Micromys minutus* (Sánchez, 1983) and *Apodemus* (*Sylvaemus*) samples have been included in the analysis for comparison purposes. (B) Bivariate plot comparing the mandibular length (ML) and coronoid height (CH) of the *Neomys* specimens from Punta Lucero III (Table S3.5) with samples from Spain and Central Europe. Sources: 1 Pemán (1983); 2 López-Fuster et al. (1990); 3 Álvarez-Vena et al. (2021); 4 Nores et al. (1982); 5 Ruprecht (1971). (C) Box and whisker plot of the distal-epiphysis breadth (Bd) of the *Lepus* humeri from Punta Lucero III compared with extant Eurasian *Lepus* samples.

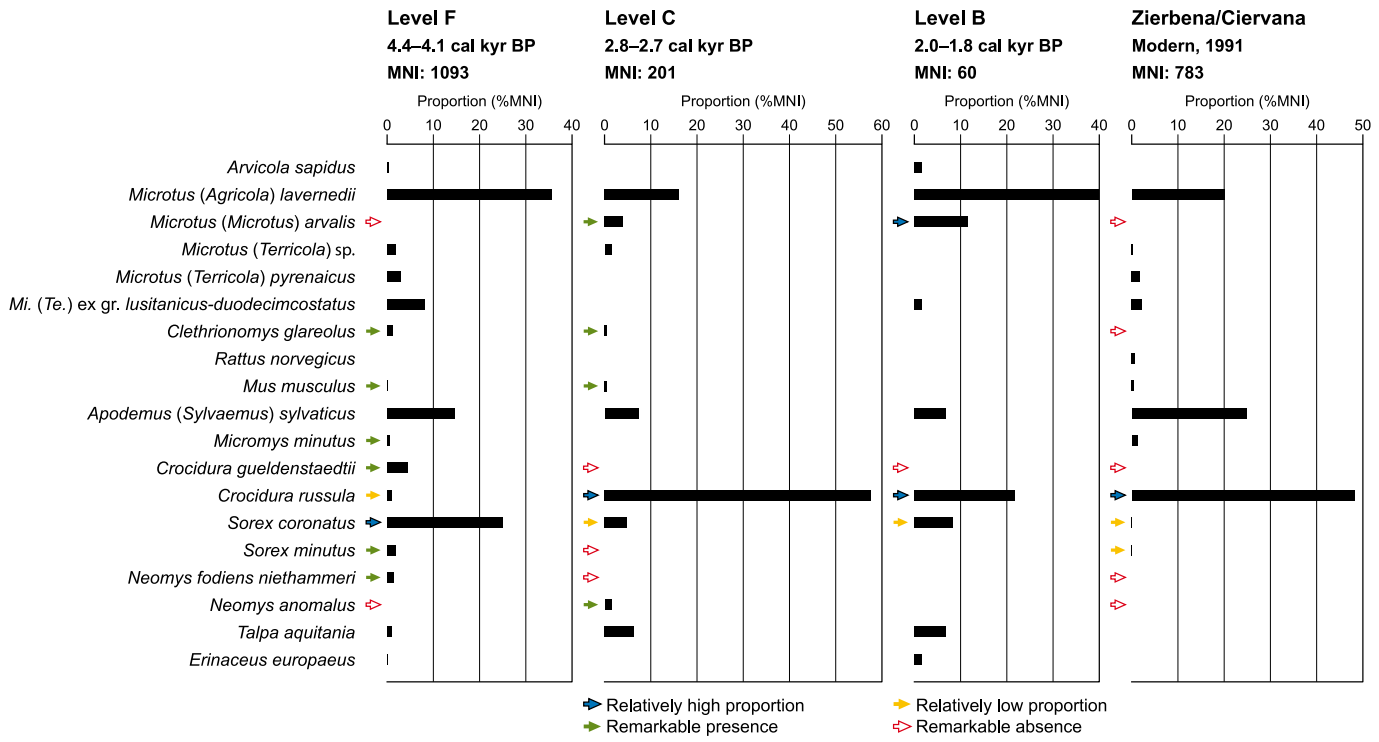

Fig. 6. Relative-abundance variations of each small-mammal species throughout the Punta Lucero III sequence compared with a modern sample from the cave surroundings. The modern sample was collected at Zierbena/Ciérvana and Somorrostro by González Oreja et al. (1993) from barn owl regurgitation pellets. Arrows indicate the species whose paleoenvironmental or paleobiogeographical significance is analysed in this work.

estimated by considering the M3, assigning the remaining individuals (since we recovered more m1 than M3) to the *Mi.* (*Terricola*) sp. denomination.

Species turnover and abundance-ratio shifts observed among the soricids of PL-III (Fig. 6) are also of paleoenvironmental significance. Based on the coronoid height (Fig. 5B; Table S3.5) and the position of the mental foramen (Fig. 4d'; Fig. 4e'), the *Neomys* sample from Level F could be assigned to *N. fodiens niethammeri* (a regional ecotype of the Eurasian water shrew) (Fig. 4d–d') while specimens from Level C correspond to *N. anomalus* (the Mediterranean water shrew) (Fig. 4e–e'). According to Palomo et al. (2007), *N. anomalus* is better adapted to Mediterranean and non-aquatic environments than *N. fodiens*, which could cause the replacement of one species by the other at Level C.

Concerning the proportion among soricines and crocidurines, in Level F, the *Sorex* genus (26.9%) surpasses *Crocidura* (5.3%), which is mainly represented by *Cr. gueldenstaedtii*, while this proportion reverses in levels C (*Crocidura*: 4.9%; *Sorex*: 57.6%) and B (*Crocidura*: 8.3%; *Sorex*: 21.7%), in which *Cr. russula* is the only crocidurine. The Güeldenstädt's white-toothed shrew (*Cr. gueldenstaedtii*), the Eurasian pygmy shrew (*Sorex minutus*), and its larger congeners at the Iberian Peninsula (*Sorex* ex gr. *coronatus-araneus*) are better adapted to humid habitats than the greater white-toothed shrew (*Cr. russula*). Both species of the genus *Crocidura* (*Cr. russula* and *Cr. gueldenstaedtii*) have been reported in sympatry at three Upper Pleistocene sites from the Cantabrian Region: El Olivo (MIS 2, Álvarez-Alonso et al., 2018), La Güelga (MIS 3, Álvarez-Vena et al., 2021), and Torca del León (MIS 3, Álvarez-Lao et al., 2020). A recent review of the Torca del León (TL) shrews by the author of the taxonomic identifications (Álvarez-Vena, A.) found that all *Crocidura* materials recovered at TL belong to the species *Cr. gueldenstaedtii*. This new datum does not affect the paleoenvironmental interpretations published by Álvarez-Lao et al. (2020) but should be considered in future paleobiogeographic studies. Among *Crocidura* species, at Level F, *Cr. gueldenstaedtii* (4.5%) is significantly more abundant than *Cr. russula* (0.8%), although it has not been registered in levels C and B, where *Cr. russula* becomes the dominant shrew (57.6% and 21.7% respectively). Nowadays, competence between both white-toothed shrews has displaced *Cr. gueldenstaedtii* to more humid environments such as marshes and wet meadows (Biedma et al., 2018, 2020). For that reason, *Cr. russula*, which can withstand drier environments, has become the dominant species in the modern micromammal associations of the cave surroundings (Fig. 8). Specimens belonging to the genus *Talpa*, when identified at the species level, are generally ascribed to two different species depending on their size: the Iberian mole (*Talpa occidentalis*) and the European mole (*Talpa europaea*). Since the recognition of a new species of the genus in the Iberian Peninsula and south of France, where the current populations of *Talpa europaea* have been ascribed to *Talpa aquitania* (Aquitanian mole) (Nicolas et al., 2015, 2017; Wilson et al., 2017), some authors started considering this new taxon, classifying the larger size moles into the *Ta.* ex gr. *europaea-aquitania* denomination (Álvarez-Lao et al., 2020; Álvarez-Vena et al., 2021). The abundant and well-preserved mole material from PL-III allowed the identification of *Ta. aquitania* in the paleontological record for the first time, after their large size (Table S3.6; Fig. S3.4) and accessory cusps in the mesostyle of the upper second and third molars (Fig. S3.3c–d').

Considering the micromammal assemblage as a whole, from Level F to Level C, there is a decreasing trend in the relative abundance of the hygrophilous and forest affinity species (*Apodemus* (*Sylvaemus*) *sylvaticus*, *Microtus* (*Agricola*) *lavernedii*, *Microtus* (*Terricola*) spp., *Crocidura gueldenstaedtii*, *Sorex minutus*, *Sorex coronatus*, and *Neomys fodiens niethammeri*), coinciding with the appearance or abundance increasing of their relative congeners with better tolerance to continental or drier conditions (*Microtus* (*Microtus*) *arvalis*, *Crocidura russula*, and *Neomys anomalus*). This trend, except for *Microtus* (*Agricola*) *lavernedii*, continued at Level B. Therefore, the observed micromammal turnover reflects a shift of the environmental conditions that took place during the formation of the respective levels: the humid and relatively forested landscape observed in Level F (4,402–4097 cal yr BP) turned into a more open and shrubbier field, especially during the accumulation of levels C (2,837–2723 cal yr BP) and B (1,992–1830 cal yr BP) (Fig. 10D). According to the inferred climatic conditions (see section 4.6), this

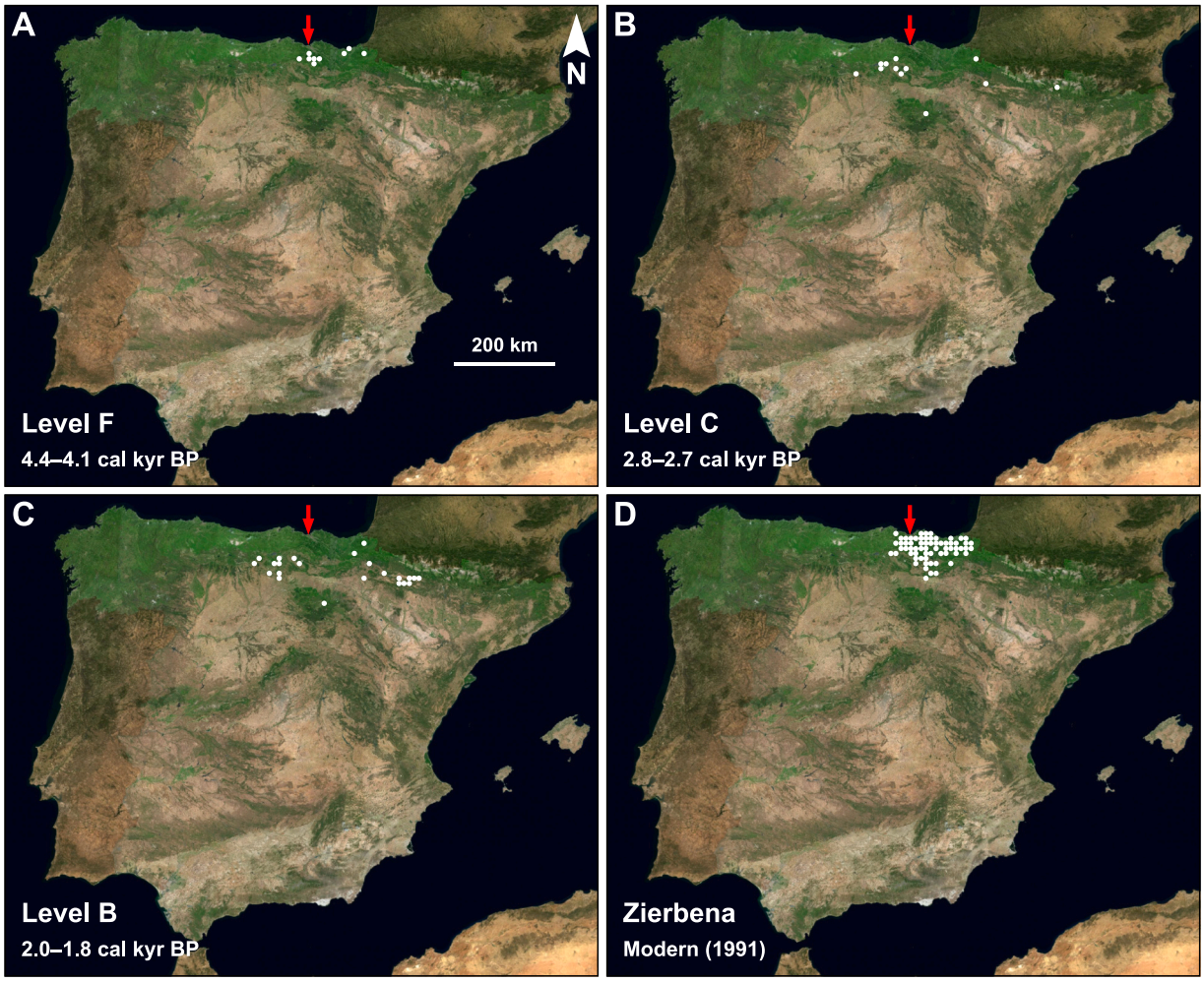

Fig. 7. Current distribution range (10 × 10 km UTM squares; Appendix 4) of the small-mammal assemblages from Levels F (A), C (B), and B (C) of the Punta Lucero sequence compared with a modern assemblage (D) collected in the cave area from regurgitation pellets by González Oreja et al. (1993). Red arrows indicate the location of the Punta Lucero III site. Base map obtained from the Spanish National Geographic Institute (http://www.ign.es/3d-stereo/). (For interpretation of the references to colour in this figure legend, the reader is referred to the web version of this article.)

Table 3
Composition of the macromammal assemblage from Punta Lucero.

	Level A		Level B		Level C		Level D		Level E		Level F	
	NISP	%NISP	NISP	%NISP	NISP	%NISP	NISP	%NISP	NISP	%NISP	NISP	%NISP
Equus sp.	3	6.52	12	12.37			1	0.32	9	2.98	15	6.91
Bos primigenius taurus	1	2.17	7	7.22	3	0.97			60	19.87	13	5.99
Capra/Ovis	42	91.30	78	80.41	276	89.03	115	36.74	74	24.50	8	3.69
Cervus elaphus							58	18.53	135	44.70	106	48.85
Capreolus capreolus							35	11.18	1	0.33	34	15.67
Sus scrofa ssp.					31	10.00	104	33.23	23	7.62	41	18.89
Total eungulate NISP*	**46**		**97**		**310**		**313**		**302**		**217**	
Canis lupus familiaris					6	26.09					17	25.76
Meles meles					17	73.91	95	100	100	100	49	74.24
Total carnivore NISP*					**23**		**95**		**100**		**66**	
Total NISP	**46**		**97**		**333**		**408**		**402**		**283**	

* The proportion of each species (%NISP) has been calculated according to the total NISP of its belonging group (eungulates or carnivores).

transformation was accompanied by an increase in the annual temperature amplitude and a decrease in the precipitations throughout the year (Fig. 11), leading to more continental climatic conditions in this coastal area. Through the isotopic study of stalagmites from the Cantabrian coast (La Garma cave, 46 km in straight-line from PL-III), Baldini et al. (2019) modelled monthly mean rainfall for the Holocene. Concerning the Late Holocene, they suggested that summers became drier from ~4.8 ka, a trend that led to very arid summers and higher-than-average annual mean precipitations at ~4.2 ka, with the current annual distribution of rainfall achieved at 1.6 ka.

Furthermore, through the study of Western Mediterranean pollen records, Jalut et al. (2000) identified aridification phases during the Holocene, which determined the changes in the vegetation cover; those contemporary to the PL-III record occurred around 5300–4200 cal yr BP,

Fig. 8. Selected ungulate specimens from Punta Lucero III. Ram (*Ovis orientalis aries*): skull from Level C with P3, M1–M3 in left lateral (a) and dorsal (a') views. Domestic goat (*Capra aegagrus hircus*): skull from Level C in right lateral (b) and dorsal (b') views; left mandible from Level C with p3–m3 series in labial (c) and occlusal (c') views; left metacarpal from Level C with unfused distal epiphyses in anterior (d) view. Cattle (*Bos primigenius taurus*): left mandible from Level E with d2, d3, d4, and m1 series in lingual (e) and occlusal (e') views; left metacarpal from Level E without unfused distal epiphyses in anterior (f) view. Red deer (*Cervus elaphus*): left metacarpal from Level E without unfused distal epiphyses in anterior (g) view. Roe deer (*Capreolus capreolus*): right maxilla from Level E with D2–M2 series in labial (h) and occlusal (h') views. Horse (*Equus* sp.): left autopodial forelimb-bones (metacarpal–distal phalanx) from Level B with some unfused epiphyses in anterior (i) view. Wild boar or swine (*Sus scrofa* ssp.): mandible from Level C with left d4 and right d3–d4 in left labial (j) and occlusal (j') views; left maxilla from Level C with d3–d4 in labial (k) view. Scale bars: 5 cm. (For interpretation of the references to colour in this figure legend, the reader is referred to the web version of this article.)

4300–3400 cal yr BP and 2850–1730 cal yr BP, the last coeval with levels C and B. Martín-Chivelet et al. (2011), through the isotopic analysis of inland stalagmites from North of Spain, reported a cold interval within this period (at 2850–2500 yr BP), matching a solar minimum and a significant perturbation in the North Atlantic circulation (Martín-Chivelet et al., 2011), though at 2500–1650 yr BP these authors identified an interval of moderate warmth. The initial cooling phase agrees with the observed at Level C; on the other hand, a slight increase in mean temperatures of Level B may correspond to the later warming period. Level C could be recording a broad chronological range since the top of the underlying Level D is dated at 3366–3185 cal yr BP and Level B dates to 1992–1830 cal yr BP. However, if Level C were recording diverse paleoenvironmental episodes, especially those moister or warmer than those reported in this work, it has not have been manifested by a recovery of the moisture indicators. Once the lasts are replaced by their better aridity-adapted congeners (e.g., *N. f.*

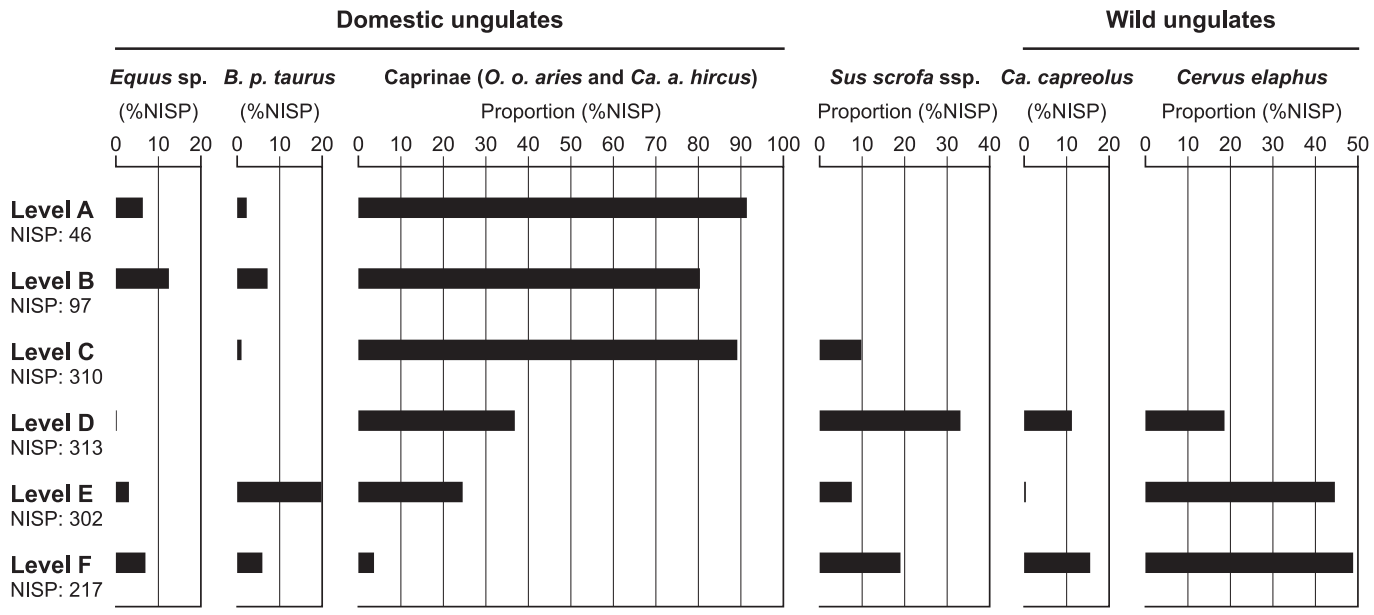

Fig. 9. Relative-abundance (%NISP) variations of each ungulate taxa throughout the Punta Lucero III sequence.

Table 4
Age at death of the macromammal assemblage.

	Infantile		Juvenile		Adult		Indet
	MNI	%	MNI	%	MNI	%	MNI
Equus sp.	4	80			1	20	
Bos primigenius taurus	3	75	1	25			2
Capra/Ovis	10	38.5	9	34.6	7	26.9	
Cervus elaphus	8	80	2	20			
Capreolus capreolus	2	40	1	20	2	40	2
Sus scrofa ssp.	11	84.6	2	15.4			
Canis lupus familiaris			1	50	1	50	1
Meles meles	10	47.6	5	23.8	6	28.6	
Total carnivores	**10**	**43.5**	**6**	**26.1**	**7**	**30.4**	**1**
Total herbivores	**38**	**60.3**	**15**	**23.8**	**10**	**15.9**	**4**
Total	**48**	**55.8**	**21**	**24.4**	**17**	**19.8**	**5**

niethammeri/N. anomalus; *Cr. gueldenstaedtii/Cr. russula*), no new records of these species are found again in the samples from this level.

On the other hand, the recovery of the relative abundance of moist indicators such as *Mi.* (*Ag.*) *lavernedii* and *So. coronatus*, along with the reappearance of *Ar. sapidus*, also agrees with the slight increase of mean temperatures of Level B (Fig. 12A). This suggests that the cooling trend could reverse during at least some phase of the accumulation of this level. Therefore, if moisture recovered during the genesis of levels C and B, it did not last enough for the main moist-adapted-faunas to return, or the anthropisation of the landscape did not enable the ecological niches of these species to recover. According to the obtained age for each level and the estimated paleoenvironmental data, levels F, C, and B represent the local expression of the climate during the Late Holocene Thermal Maximum, the Iron Age Cold Epoch, and the Roman Warm Period, respectively (Fig. 10; Fig. 12). Reconstruction of the landscape in which Level D accumulated also suggests moister conditions for this level than the registered in levels C and B. This is in concordance with the dating of Level D within the Bronze Age Optimum, a warm period that also has been recorded in other coetaneous micromammal assemblages from northern Iberia (e.g., Bañuls-Cardona et al., 2013; Ordiales et al., 2015).

5.3. Mammalian turnover in response to anthropogenic causes

The environmental transformation recorded at the PL-III sequence, from a mosaic of forest patches and humid meadows into drier and bushier pastures, was also accompanied by a change in the macromammal species associations (Fig. 9; Fig. 10E). Wild herbivores with forest affinity such as cervids (*Cervus elaphus* and *Capreolus capreolus*), account for 83% of ungulate NISP from Level F, 53% of Level E and 63% of Level D. These taxa are absent at levels C and B. Contrariwise, the group of domestic grazers, such as bovids (*Ovis orientalis aries*, *Capra aegagrus hircus* and *Bos primigenius taurus*) and equids (*Equus* sp.), which are represented at all levels, increases from the bottom (17% of the ungulate NISP from Level F) to the top (100% of the ungulate NISP from Level B) of the sequence. The oldest evidence of livestock at the Cantabrian Region, consisting of *Bos primigenius taurus* (cattle) bones, come from the Neolithic occupations at Arenaza (~11 km south of PL-III) and date from 7157 to 6401 cal yr BP (Altuna and Arias Cabal, 1999). Also, the first evidence of agriculture in the area, determined from charred cereals, is chronologically coeval (Zapata Peña, 1999, 2002; Zapata Peña et al., 2005; Peña-Chocarro et al., 2005; Iriarte et al., 2005). According to pollen records, the decline and disturbance of Cantabrian forests due to anthropogenic causes, which started at ~7.3–6.5 ka in agreement with the first Neolithic farming evidence mentioned above, progressively increased from the Metal Ages onwards (Ramil-Rego et al., 1998; Muñoz Sobrino et al., 2005; López Merino, 2009; López-Merino et al., 2010; Pérez-Obiol et al., 2016; Pérez-Díaz et al., 2016, 2018; Carracedo et al., 2018). The use of fire for maintenance of pasture areas after forest clearance (e.g., Carracedo et al., 2018; Pérez-Obiol et al., 2016) led to forests being replaced by shrub-like communities, generally, thickets dominated by heathers (Ramil-Rego et al., 1998; López Merino, 2009; Pérez-Díaz et al., 2018). Evidence of such practices and landscape transformations have been recorded at PL-III in the form of abundant charcoal fragments, especially at the lower half of the sequence (levels F—D). Furthermore, the relative abundance of micromammals adapted to this kind of anthropogenic landscape (OD: dry grasslands and shrublands) significatively increased at levels C and B of PL-III, which are coeval with the Iron Age and Roman Empire, respectively (Fig. 10; Fig. 12). Therefore, all this evidence points to an increasing anthropisation of the site surroundings for its adaptation to livestock practices. Micromammal assemblages studied at coeval deposits of northern Iberia, such as El Mirador (Burgos), Valdavara-1 (Galicia), or Cova Colomera (Lleida), also indicate a similar timing for the increase of anthropogenic pressure over the terrestrial ecosystems (Bañuls-Cardona and López-García, 2016; Bañuls-Cardona et al., 2017b).

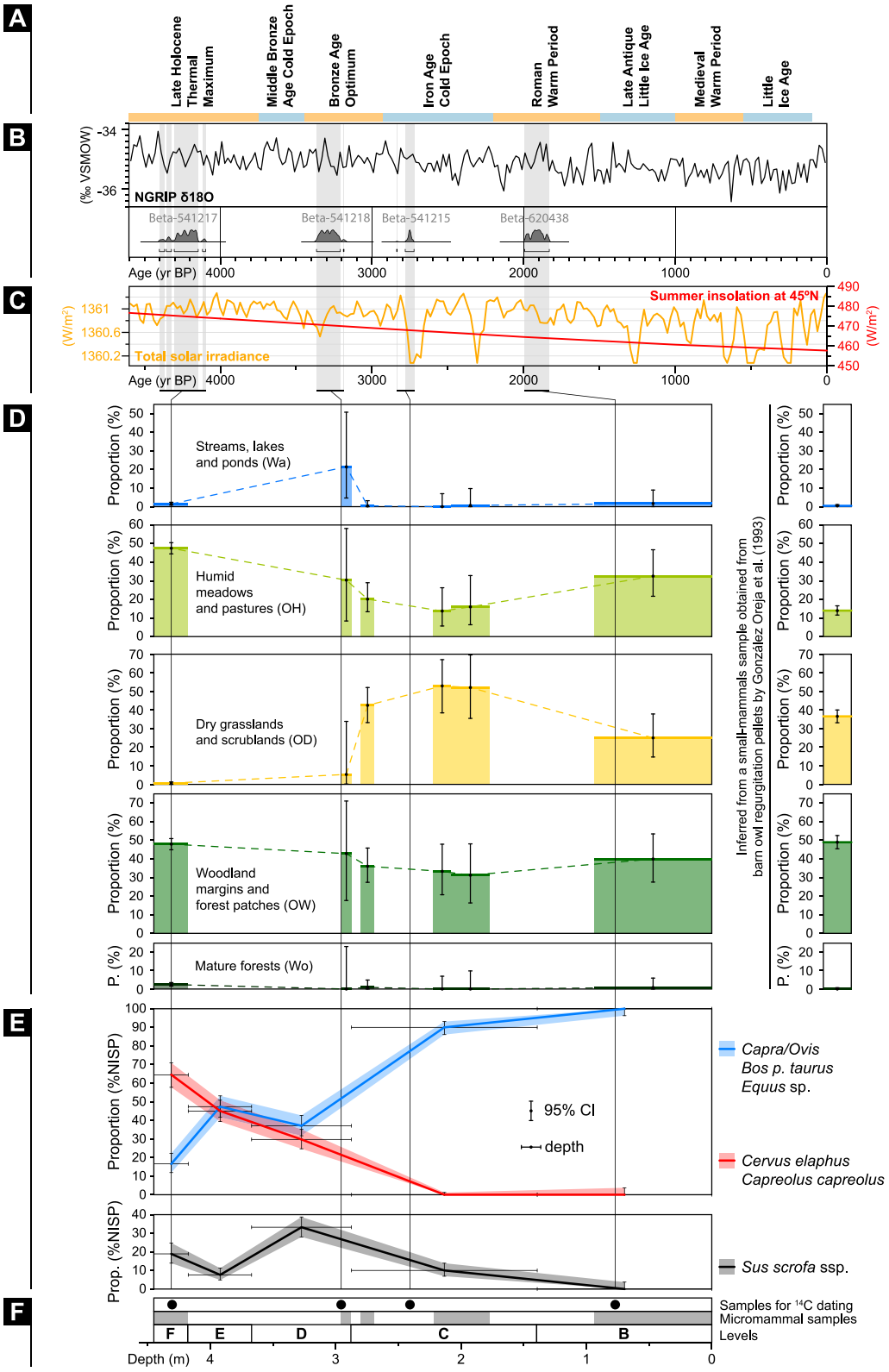

Fig. 10. Contextualisation of the environmental and anthropic influence on the mammal community of Punta Lucero III. (A) List of climatic episodes associated with the studied chronological range. (B) NGRIP $\delta^{18}O$ curve (Andersen et al., 2004) compared with the radiocarbon dates obtained for the Punta Lucero shaft sequence. (C) Graphic representing total solar irradiance reconstruction (Steinhilber et al., 2012) versus summer insolation at 45°N (Laskar et al., 2004). (D) Type of landscape evolution at the surroundings of the Punta Lucero III shaft inferred through the Habitat Weighting method. (E) Compared relative-abundance variations of wild and domestic ungulates throughout the Punta Lucero III sequence. *Sus scrofa* ssp. abundance is plotted separately since this taxon comprises a wild (*Sus scrofa scrofa*: wild boar) and a domestic species (*Sus scrofa domestica*: pig). (F) The depth scale indicates each level's stratigraphic position, the origin of each sediment sample for water screening, and the provenance of the radiocarbon dating samples. A–C graphs are plotted according to the age scale. D–F graphs are plotted according to the depth scale. The multiple proportion 95% confidence intervals (CI) have been obtained using the Clopper-Pearson Method (Clopper and Pearson, 1934) using the PAST 4.0 software (Hammer et al., 2001).

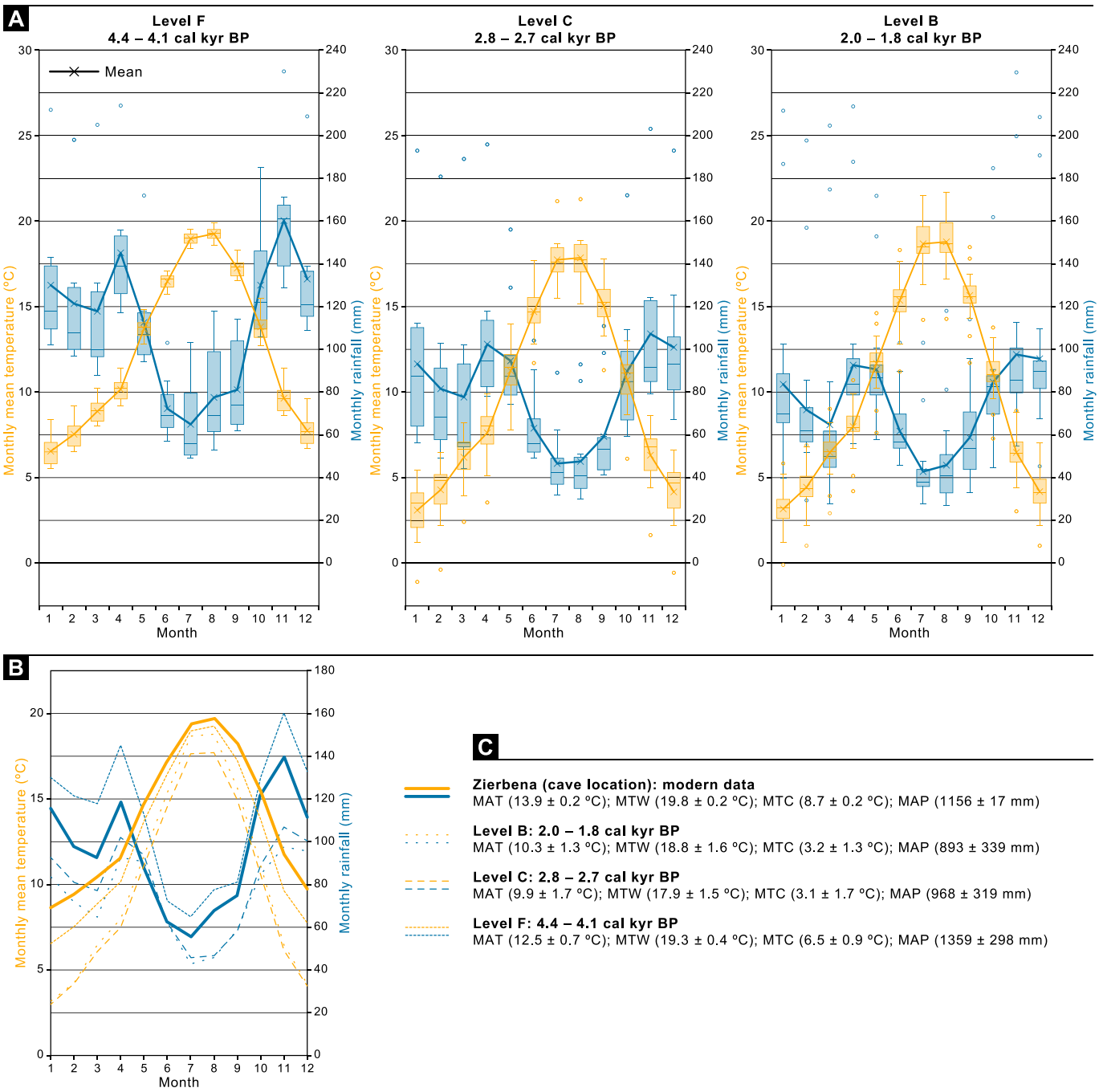

Fig. 11. Temperature and rainfall estimations based on the Mutual Ecogeographic Range method. (A) Box and whisker plot of the monthly values obtained through the Mutual Ecogeographic Range method (Appendix 4) for each micromammal association of the Punta Lucero III sequence (levels F, C, and B). (B) Monthly mean values of estimated temperature and rainfall from levels F, C, and B compared with present-day data from the Punta Lucero III location. (C) Mutual Ecogeographic Range method estimations: mean annual temperature (MAT), mean temperature of the warmest month (MTW), mean temperature of the coldest month (MTC), mean annual precipitation (MAP).

From ~5 ka, steppe pastoralists of the Yamnaya culture expanded east- and westward, linking Asia and Europe (Allentoft et al., 2015; Lazaridis et al., 2022). This created a geographic corridor which, aided by the development of horse-riding and chariotry (Anthony, 2007; Anthony and Brown, 2011; Wilkin et al., 2021), led to the dispersal of crops, herds, and commensal species from one continent to another. Regarding the Iberian Peninsula, an increasing gene inflow from Northern and Central European human populations with steppe ancestry has been detected (Olalde et al., 2019; Villalba-Mouco et al., 2021; Patterson et al., 2022), dating the earliest evidence from ~4.5–4 ka, from individuals who coexisted with locals without steppe ancestry (Olalde et al., 2019). This incoming pastoralist peopling to the region agrees with the increasing anthropic pressure linked to animal husbandry observed at PL-III and the coeval records mentioned. However, the increase in domestic herds and deforestation is not the only way those migrations are perceived in the PL-III deposit. The harvest mouse (*Micromys minutus*), identified at Level F, and the house mouse (*Mus musculus*), found at levels F and C, are reported from PL-III at a significantly early chronology. According to Horáček et al. (2013), Pliocene and Pleistocene European records previously ascribed to the *Micromys* genus belong to *Parapodemus coronensis* Schaub, 1930, which did not have continuity in the Late Pleistocene. This agrees with the work of

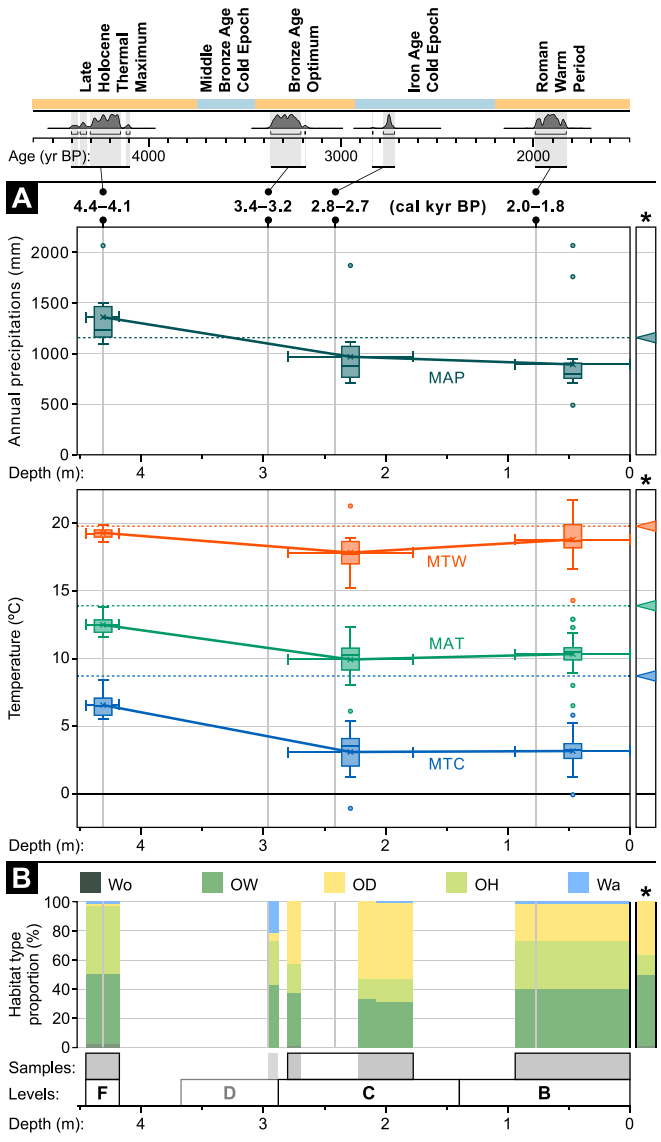

Fig. 12. Compared paleoclimatic and paleoenvironmental reconstructions of the Punta Lucero III sequence. (A) Mutual Ecogeographic Range estimations of levels F, C, and B: mean annual precipitation (MAP), mean temperature of the warmest month (MTW), mean annual temperature (MAT), mean temperature of the coldest month (MTC). Dash lines and asterisk columns indicate the present-day values obtained from the Iberian Climate Atlas (Couto et al., 2011). (B) Type of landscape evolution at the surroundings of the Punta Lucero III shaft inferred through the Habitat Weighting method. Levels and samples are plotted according to depth. The column with an asterisk corresponds to a modern micromammal sample collected in the Punta Lucero area from barn owl regurgitation pellets by González Oreja et al. (1993).

Yasuda et al. (2005), who, based on the phylogeographic pattern of mtDNA, propose that the extant species originated in East Asia. The fossil record suggests that *Micromys minutus* reached Europe during the Holocene (e.g., Mistrot, 2011, 2013a, 2013b; Serjeantson, 2011; Krajcarz et al., 2020; Royer et al., 2021), but the scarcity of reliable records to date does not allow us to reconstruct a precise timing. Concerning the Iberian Peninsula, the species has been identified at two different sites: Level 2 of Valdavara-1 (Lugo, Galicia; 5305–4978 cal yr BP; López-García et al., 2011) and Level 1 of Amalda (Gipuzkoa, Basque Country; Pemán, 1990), which yielded three dates ranging from 3875 to 1179 cal kyr BP (the oldest considered aberrant by Altuna, 1990). Considering the measurements published in López-García et al. (2011), the material ascribed to *Micromys minutus* in Valdavara-1 falls in size with small specimens of *Apodemus sylvaticus* (Fig. 5A), which could indicate that it is this species and not the previous one, in the absence of reviewing the identified material. This means that the reported in this work could be the oldest record of this species in the Iberian Peninsula.

The spread of the harvest mouse across Eurasia was probably boosted by the development of agriculture, especially by millet crops, which, conversely to other cereals, do not belong to the first set of Neolithic crops from the Middle East. Instead, this cereal was initially domesticated in north-eastern China at ~8 ka (Liu et al., 2004; Crawford et al., 2013) and later spread to the rest of Central Eurasia and Eastern Europe (Miller et al., 2016; Filipović et al., 2020). Foxtail millet (*Setaria italica*), among other remains of cereals, has been found at the nearby sites of Kobaederra (Level 1) and Arenaza (Level 9) at 5280–4855 cal yr BP and 4085–3693 cal yr BP respectively (Zapata Peña, 1999, 2002). Therefore, the harvest mouse occurrence at PL-III (Level F: 4402–4097 cal yr BP) and the arrival of millet crops to the region share similar chronological ranges. The earliest evidence of millet consumption by humans in the Cantabrian Region (3163–3051 cal yr BP) has been documented at El Espinoso (Asturias; González-Rabanal et al., 2022) at ~100 km west of PL-III by individuals with a significant proportion of steppe ancestry (30%, Patterson et al., 2022). Therefore, steppe migrations could be related to harvest mouse arrival in the Cantabrian Region.

About the house mouse (*Mus musculus*), its record in southwestern Europe has been reviewed by Cucchi et al. (2005) and Domínguez García et al. (2019), who found that most of the reports of the species lack published reliable identifications or come from unclear contexts. Even new data from the Cantabrian Region published by Martínez-Villa et al. (2022) and Cernadas-Garrido et al. (2023) may correspond to intrusive specimens and materials of mixed–chronology, respectively. The earliest evidence of *Mus musculus domesticus* in Iberia comes from Iron Age at the Alorda Parc site (Valenzuela-Lamas et al., 2011). Domínguez García et al. (2019) also place the earliest reliable presence of the house mouse at the Iberian Peninsula within the Iron Age, at ~3 ka, supporting the hypothesis of a dispersal linked to the increase in the sea trade between eastern and western Mediterranean (Cucchi et al., 2005), driven by the commercial expansion of the Phoenicians and Greeks (Cucchi et al., 2012). The oldest records of the house mouse (*Mus musculus musculus*) from inland Europe come from Eastern Europe and date from the end of the Neolithic (~6.5 ka; Cucchi et al., 2011, 2020). Based on this unexpected finding, Cucchi et al. (2012) proposed a centre of synanthropization for this subspecies in eastern Europe north of the Black Sea. Therefore, a route from the steppes through inland Europe could be an alternative pathway for the arrival of *Mus musculus* to the Cantabrian Region. This is consistent with the reliable finding of *Mus musculus* ssp. in northern Italy (Tosina, Milan) dated at ~6 ka (Bona, 2020). However, further research and direct radiocarbon dating of the PL-III specimens need to be done to avoid misinterpretation of this record.

Table 5
Proportion (%) of skeletal remains showing carnivore tooth marks.

	Level A	Level B	Level C	Level D	Level E	Level F	Total
NSP*	46	188	414	989	707	876	**3220**
Tooth-marked specimens	0	17	51	45	42	46	**201**
Frequency (%)	0	9	12.3	4.6	5.9	5.3	**6.2**

* Number of specimens (includes specimens that cannot be identified to taxon).

Table 6
Weighted (%) habitat-preferences[a] with 95% confidence intervals[b] of the small mammal assemblage from each level of Punta Lucero.

	MNI	Wa	OD	OH	OW	Wo
Zierbena modern (González-Oreja et al., 1993)	773	0.00	36.58	13.71	49.61	0.10
95% CI		0.00–0.48	33.21–40.12	11.37–16.34	45.97–53.13	0.00–0.72
Level B (Sample z: 0–93)	60	1.67	25.00	32.50	40.00	0.83
95% CI		0.04–8.94	14.72–37.86	21.69–46.69	27.56–53.46	0.00–5.96
Level C-upper (Sample z: 208–177)	36	0.69	52.08	15.97	31.25	0.00
95% CI		0.00–9.74	35.49–69.59	6.37–32.81	16.35–48.11	0.00–9.74
Level C-middle (Sample z: 222–208)	51	0.00	52.94	13.73	33.33	0.00
95% CI		0.00–6.98	38.46–67.07	5.70–26.26	20.76–47.92	0.00–6.98
Level C-bottom (Sample z: 280–269)	113	0.44	42.48	20.13	36.06	0.88
95% CI		0.00–3.21	33.23–52.13	13.36–28.96	27.45–45.86	0.02–4.83
Level D (Sample z: 296–288)	14	21.43	5.36	30.36	42.86	0.00
95% CI		4.66–50.80	0.18–33.87	8.39–58.10	17.66–71.14	0.00–23.16
Level F (Sample z: 445–420)	1092	1.47	0.62	47.50	47.99	2.43
95% CI		0.84–2.37	0.26–1.32	44.53–50.54	44.99–51.00	1.64–3.58

[a] Wa, water; OH, open humid; OD, open dry; OW, open woodland; Wo, woodland.
[b] 95% CI: multiple proportions 95% confidence intervals calculated using the Clopper-Pearson method (Clopper and Pearson, 1934) using the PAST 4.0 software (Hammer et al., 2001).

6. Conclusions

The mammal assemblage studied in this work was mainly produced by accidental falling in the PL-III cave, which acted as a natural trap through time. Nocturnal birds of prey could also be implied in the accumulation of the micromammal assemblage since our analyses did not allow us to rule out these predators. The studied samples provided a large number of remains corresponding to 18 micromammal and nine macromammal taxa. Micromammal community underwent a quick turnover which reflects a shift of the environmental conditions that took place during the formation of the deposit: the moist mosaic of forest and meadows observed in Level F (4,402–4097 cal yr BP) turned into an open and shrubbier grassland during the accumulation of levels C (2,837–2723 cal yr BP) and B (1,992–1830 cal yr BP). The earliest Iberian records of *Mus musculus* and, most likely, of *Micromys minutus* here reported could be related to the dispersal of the steppe pastoralist. Still, direct radiocarbon dating needs to be done to obtain a more precise date for these remains. Simultaneously, macromammals experienced a shift from wild populations to domestic herds, which, along with the abundant charcoal fragments recovered in the sediment, suggest that anthropogenic fires for the development of livestock pastures caused forest disappearance and did not allow them to recover. Temperature and rainfall estimations reveal that the humid and mild climatic conditions observed at the bottom of the sequence, which occurred during the Late Holocene Thermal Maximum, went through a cooling and aridification phase, coeval with the Iron Age Cold Epoch, and concluded in a slight warming, coeval with the Roman Warm Period.

Declaration of Competing Interest

The authors declare that they have no known competing financial interests or personal relationships that could have appeared to influence the work reported in this paper.

Data availability

No data was used for the research described in the article.

Acknowledgements

AB.M-A. developed part of this research as part of the ERC Consolidator Grant (SUBSILIENCE ref. 818299). We thank J.A. Delgado for his technical work on studying macromammal assemblage. Financial support was provided by the Bilbao Port Authority (Autoridad Portuaria de Bilbao) within the project “Estabilización del sector occidental de la Cantera de Punta Lucero en el Puerto de Bilbao”. We are also grateful to Juan Manuel López-García and the anonymous reviewer for their suggestions and comments that strongly improved the manuscript.

Appendix A. Supplementary data

Supplementary data to this article can be found online at https://doi.org/10.1016/j.palaeo.2023.111476.

References

Allentoft, M., Sikora, M., Sjögren, K.G., et al., 2015. Population genomics of Bronze Age Eurasia. Nature 522, 167–172.
Alley, R.B., Mayewski, P.A., Sowers, T., Stuiver, M., Taylor, K.C., Clark, P.U., 1997. Holocene climatic instability: a prominent, widespread event 8200 yr ago. Geology 25, 483–486.
Altuna, J., 1980. Historia de la domesticación animal, en el País Vasco, desde sus orígenes hasta la romanización. Munibe 30, 1–163.
Altuna, J., 1990. Situación y descripción de la cueva de Amalda. Historia de las excavaciones. Descripción del relleno. Estructuras en el yacimiento. Dataciones de radiocarbono. Otros yacimientos del valle. In: La cueva de Amalda (Zestoa, País Vasco): ocupaciones paleolíticas y postpaleolíticas, pp. 9–31. Colección Barandiaran (4). Eusko Ikaskuntza.
Altuna, J., Arias Cabal, P., 1999. Nuevas dataciones absolutas Para el Neolítico de la Cueva de Arenaza (Bizkaia). Munibe (Antropologia-Arkeologia) 51, 161–171.
Altuna, J., Mariezkurrena, K., 2012. Macromammalian remains from the Holocene levels of El Mirón Cave. In: Straus, L.G., González Morales, M. (Eds.), El Mirón Cave, Cantabrian Spain. University of New Mexico Press, Albuquerque, pp. 288–318.
Álvarez-Alonso, D., Álvarez-FernÁndez, E., de Andrés-Herrero, M., Ballesteros, D., García-Ibaibarriaga, N., Jiménez-SÁnchez, M., JordÁ-Pardo, J.F., Yravedra, J., 2018. Excavaciones en la Cueva del Olivo (Pruvia, Llanera). Campañas 2013–2016. Excavaciones Arqueológicas en Asturias 2013–2016, 121–132.
Álvarez-Lao, D.J., 2014. The Jou Puerta cave (Asturias, NW Spain): a MIS 3 large mammal assemblage with mixture of cold and temperate elements. Palaeogeogr. Palaeoclimatol. Palaeoecol. 393, 1–19.
Álvarez-Lao, D.J., Álvarez-Vena, A., Ballesteros, D., García, N., Laplana, C., 2020. A cave lion (Panthera spelaea) skeleton from Torca del León (NW Iberia): micromammals indicate a temperate and forest environment corresponding to GI-11 (MIS 3). Quat. Sci. Rev. 229, 106123.
Álvarez-Vena, A., Álvarez-Lao, D.J., Laplana, C., Quesada, J.M., Rojo, J., García-Sánchez, E., Menéndez, M., 2021. Environmental context for the late Pleistocene

(MIS 3) transition from neanderthals to early modern humans: analysis of small mammals from La Güelga Cave, Asturias, northern Spain. Palaeogeogr. Palaeoclimatol. Palaeoecol. 562, 110096.
Andersen, K.K., Azuma, N., Barnola, J.M., et al., 2004. High resolution climate record of the Northern Hemisphere reaching into the last glacial interglacial period. Nature 431, 147–151.
Andrews, P., 1990. Owls, Caves and Fossils. Predation, Preservation and Accumulation of Small Mammal Bones in Caves, With an Analysis of the Pleistocene Cave Faunas from Westbury-sub-Mendip. The University of Chicago Press, Somerset, UK, London.
Andrews, P., 2006. Taphonomic effects of faunal impoverishment and faunal mixing. Palaeogeogr. Palaeoclimatol. Palaeoecol. 241, 572–589.
Anthony, D.W., 2007. The Horse, the Wheel, and Language: How Bronze-Age Riders from the Eurasian Steppes Shaped the Modern World. Princeton University Press.
Anthony, D.W., Brown, D.R., 2011. The secondary products revolution, horse-riding, and mounted warfare. J. World Prehist. 24, 131.
Aranburu, A., Arriolabengoa, M., Iriarte, E., Giralt, S., Yusta, I., Martínez-Pillado, V., del Val, M., Moreno, J., Jiménez-Sánchez, M., 2015. Karst landscape evolution in the littoral area of the Bay of Biscay (north Iberian Peninsula). Quat. Int. 364, 217–230.
Arriolabengoa, M., Iriarte, E., Aranburu, A., Yusta, I., Arrizabalaga, A., 2015. Provenance study of endokarst fine sediments through mineralogical and geochemical data (Lezetxiki II cave, northern Iberia). Quat. Int. 364, 231–243.
Arilla, M., Rufà, A., Rosell, J., Blasco, R., 2020. Small carnivores' cave-dwelling: neo-taphonomic study of a badger (Meles meles) sett and its archaeological implications. Hist. Biol. 32 (7), 951–965.
Azorit, E., Analla, M., Carrasco, R., Calvo, J.A., Muñoz-Cobo, J., 2002. Teeth eruption pattern in red deer (Cervus elaphus hispanicus) in southern Spain. Anales de Biología 24, 107–114.
Baldini, L.M., Baldini, J.U.L., McDermott, F., Arias, P., Cueto, M., Fairchild, I.J., Hoffmann, D.L., Mattey, D.P., Müller, W., Nita, D.C., Ontañón, R., García-Moncó, C., Richards, D.A., 2019. North Iberian temperature and rainfall seasonality over the Younger Dryas and Holocene. Quat. Sci. Rev. 226, 105998.
Ballesteros, D., Álvarez-Vena, A., Monod-Del Dago, M., Rodríguez-Rodríguez, L., Sanjurjo-Sánchez, J., Álvarez-Lao, D., Pérez-Mejías, C., Valenzuela, P., DeFelipe, I., Laplana, C., Cheng, H., Jiménez-Sánchez, M., 2020. Paleoenvironmental evolution of Picos de Europa (Spain) during marine isotopic stages 5c to 3 combining glacial reconstruction, cave sedimentology and paleontological findings. Quat. Sci. Rev. 248, 106581.
Bañuls-Cardona, S., López-García, J.M., 2016. Climatic and environmental conditions from the Neolithic to the Bronze Age (7000–3000 BP) in the Iberian Peninsula assessed using small-mammal assemblages. Comptes Rendus Palevol 15, 958–967.
Bañuls-Cardona, S., López-García, J.M., Vergès, J.M., 2013. Palaeoenvironmental and palaeoclimatic approach of the middle bronze age (level MIR 4) from El Mirador Cave (Sierra de Atapuerca, Burgos, Spain). Quaternaire 24 (2), 217–223.
Bañuls-Cardona, S., López-García, J.M., Morales Hidalgo, J.I., Cuenca-Bescós, G., Vergès, J.M., 2017a. Lateglacial to late Holocene palaeoclimatic and palaeoenvironmental reconstruction of El Mirador cave (Sierra de Atapuerca, Burgos, Spain) using the small-mammal assemblages. Palaeogeogr. Palaeoclimatol. Palaeoecol. 471, 71–81.
Bañuls-Cardona, S., Martín Rodríguez, P., López-García, J.M., Morales, J.I., Cuenca-Bescós, G., Vergès, J.M., 2017b. Human impact on small-mammal diversity during the middle- to late-Holocene in Iberia: the case of El Mirador cave (Sierra de Atapuerca, Burgos, Spain). The Holocene 27 (8), 1067–1077.
Baraybar, J.P., de la Rúa, C., 1995. Anthropological study of the population of Pico Ramos (Muskiz, Biscay). Some considerations regarding demography, health and subsistence. In: Zapata, L. (Ed.), The Chalcolithic burial deposit of the cave Pico Ramos (Muskiz, Biskay). Munibe (Antropologia-Arkeologia) 47, pp. 151–175.
Barnosky, A.D., 2008. Megafauna biomass tradeoff as a driver of quaternary and future extinctions. Proceedings of the National Academy of Sciences 105 (1), 11543–11548.
Barnosky, A.D., 2013. Palaeontological evidence for defining the Anthropocene. Geol. Soc. Lond. Spec. Publ. 395 (1), 149–165.
Barone, R., 1976. Anatomie comparée des mammifères domestiques. Tome I Ostéologie, Vigot Fréres Editeurs, París.
Barti, L., 2006. Az állkapcsi lyuk (Foramen mentale) helyzete mint kiegészítő határozóbélyeg a Neomys fajok (Mammalia, Insectivora Soricidae) biztosabb elkülönítésére. Acta Siculica 1, 191–199.
Beck, H.E., Zimmermann, N.E., McVicar, T.R., Vergopolan, N., Berg, A., Wood, E.F., 2018. Present and future Köppen-Geiger climate classification maps at 1-km resolution. Sci. Data 5, 180214.
Biedma, L., Román, J., Calzada, J., Friis, G., Godoy, J.A., 2018. Phylogeography of Crocidura suaveolens (Mammalia: soricidae) in Iberia has been shaped by competitive exclusion by C. Russula. Biol. J. Linn. Soc. 123 (1), 81–95.
Biedma, L., Calzada, J., Godoy, J.A., Román, J., 2020. Local habitat specialization as an evolutionary response to interspecific competition between two sympatric shrews. J. Mammal. 101 (1), 80–91.
Binford, L.R., 1981. Bones. Ancient Men and Modern Myths, Studies in Archaeology. Academic Press, New York.
Blain, H.-A., Bailon, S., Cuenca-Bescós, G., 2008. The Early-Middle Pleistocene palaeoenvironmental change based on the squamate reptile and amphibian proxies at the Gran Dolina site, Atapuerca, Spain. Palaeogeogr. Palaeoclimatol. Palaeoecol. 261, 177–192.
Blain, H.-A., Bailon, S., Cuenca-Bescós, G., Arsuaga, J.L., Bermúdez de Castro, J.M., Carbonell, E., 2009. Long-term climate record inferred from early-middle Pleistocene amphibian and squamate reptile assemblages at the Gran Dolina Cave, Atapuerca, Spain. J. Hum. Evol. 56 (1), 55–65.
Blain, H.-A., Lozano-Fernández, I., Agustí, J., Bailon, S., Menéndez, L.G., Espígares, P.O. M., Ros-Montoya, S., Jiménez, J.M.A., Toro-Moyano, I., Martínez-Navarro, B., Sala, R., 2016. Refining upon the climatic background of the Early Pleistocene hominid settlement in western Europe: Barranco León and Fuente Nueva-3 (Guadix-Baza Basin, SE Spain). Quat. Sci. Rev. 144, 132–144.
Boivin, N.L., Zeder, M.A., Fuller, D.Q., Crowther, A., Larson, G., Erlandson, J.M., Denham, T., Petraglia, M.D., 2016. Ecological consequences of human niche construction: Examining long-term anthropogenic shaping of global species distributions. Proc. Nat. Acad. Sci. 113 (23), 6388–6396.
Bona, F., 2020. . Earliest evidence of Mus musculus ssp. in Western Europe during the Late Neolithic (Tosina, Mantova, Northern Italy): new insights on the house mice migratory waves. Hystrix Ital. J. Mammal. 31 (2), 111–116.
Bond, G., Showers, W., Cheseby, M., Lotti, R., Almasi, P., deMenocal, P., Priore, P., Cullen, H., Hajdas, I., Bonani, G., 1997. A pervasive millennial-scale cycle in North Atlantic Holocene and glacial climates. Science 278 (5341), 1257–1266.
Bond, G., Kromer, B., Beer, J., Muscheler, R., Evans, M., Showers, W., Hoffmann, S., Lotti-Bond, R., Hajdas, I., Bonani, G., 2001. Persistent solar influence on North Atlantic climate during the Holocene. Science 294, 2130–2136.
Borzenkova, I., Zorita, E., Borisova, O., Kalniņa, L., Kisielienė, D., Koff, T., Kuznetsov, D., Lemdahl, G., Sapelko, T., Stančikaitė, M., Subetto, D., 2015. Climate change during the Holocene (Past 12,000 Years). In: The BACC II Author Team, (Eds) Second Assessment of Climate Change for the Baltic Sea Basin. Regional Climate Studies. Springer, Cham, pp. 25–49.
Bray, J.R., 1971. Solar–climate relationships in the post-Pleistocene. Science 171, 1242–1243.
Bronk Ramsey, C., 2009. Bayesian analysis of radiocarbon dates. Radiocarbon 51 (1), 337–360.
Büntgen, U., Tegel, W., Nicolussi, K., McCormick, M., Frank, D., Trouet, V., Kaplan, J.O., Herzig, F., Heussner, K.-U., Wanner, H., Luterbacher, J., Esper, J., 2011. 2500 years of European climate variability and human susceptibility. Science 331 (6017), 578–582.
Carracedo, V., Cunill, R., García-Codron, J.C., Pèlachs, A., Pérez-Obiol, R., Soriano, J.M., 2018. History of fires and vegetation since the Neolithic in the Cantabrian Mountains (Spain). Land Degrad. Dev. 29 (7), 2060–2072.
Carrión, J.S., Fernández, S., González-Sampériz, P., Gil-Romera, G., Badal, E., Carrión-Marco, Y., López-Merino, L., López-Sáez, J.A., Fierro, E., Burjachs, F., 2010. Expected trends and surprises in the Lateglacial and Holocene vegetation history of the Iberian Peninsula and Balearic Islands. Rev. Palaeobot. Palynol. 162, 458–475.
Castaños, P., 1997. Estudio arqueozoológico de la fauna de Peña Larga (Cripán, Álava). In: Fernández Eraso, J. (Ed.), Peña Larga: memoria de las excavaciones arqueológicas 1985–1989. Memorias de yacimientos alaveses. n° 4. Diputación Foral de Álava, Vitoria-Gasteiz, pp. 127–134.
Cernadas-Garrido, A., Álvarez-Vena, A., Álvarez-Lao, D.J., 2023. Palaeobiological study of the Holocene micromammal assemblage from the Cueva del Hueso (Castrillón, Asturias, NW Spain). Spanish J. Palaeontol. 38 (1) https://doi.org/10.7203/sjp.25962 in press.
Clopper, C.J., Pearson, E.S., 1934. The use of confidence or fiducial limits illustrated in the case of the binomial. Biometrika 26 (4), 404–413.
Couto, M.A., Sánchez, G., Tavares, C.D., Barceló, A.M., Nunes, L.F., Herráez, C.F., Pires, V., Marques, J., Mendes, L., Chazarra, A., Cunha, S., Mendes, M., Neto, J., Silva, A., 2011. Atlas Climático Ibérico-Iberian Climate Atlas. Instituto de Meteorologia de Portugal and Agencia Estatal de Meteorología, Ministerio de Medio Ambiente y Medio Rural y Marino (Eds.).
Crawford, G.W., Chen, X., Luan, F., 2013. A preliminary analysis of plant remains from the Yuezhuang site, Changqing district, Jinan, Shandong province. Jianghan Kaogu (2), 107–113.
Crutzen, P.J., 2002. Geology of mankind. Nature 415, 23.
Cucchi, T., Vigne, J.-D., Auffray, J.-C., 2005. First occurrence of the house mouse (Mus musculus domesticus Schwarz & Schwarz, 1943) in the Western Mediterranean: a zooarchaeological revision of subfossil occurrences. Biol. J. Linn. Soc. 84, 429–445.
Cucchi, T., Bălăşescu, A., Bem, C., Radu, V., Vigne, J.-D., Tresset, A., 2011. New insights into the invasive process of the eastern house mouse (Mus musculus musculus): evidence from the burnt houses of Chalcolithic Romania. The Holocene 21 (8), 1195–1202.
Cucchi, T., Auffray, J.-C., Vigne, J.-D., 2012. On the origin of the house mouse synanthropy and dispersal in the Near East and Europe: zooarchaeological review and perspectives. In: Macholán, M., Baird, S.J.E., Munclinger, P., Piálek, J. (Eds.), Evolution of the House Mouse. Cambridge Studies in Morphology and Molecules: New Paradigms in Evolutionary Biology. Cambridge University Press, Cambridge, pp. 65–93.
Cucchi, T., Papayianni, K., Cersoy, S., et al., 2020. Tracking the near Eastern origins and European dispersal of the western house mouse. Sci. Rep. 10, 8276.
Cuenca-Bescós, G., Straus, L.G., González Morales, M., García Pimineta, J.C., 2009. The reconstruction of past environments through small mammals: from the Mousterian to Bronze Age in El Mirón cave (Cantabria, Spain). J. Archaeol. Sci. 36, 947–955.
Cuenca-Bescós, G., Marín-Arroyo, A.B., Martínez, I., González Morales, M.R., Straus, L. G., 2012. Relationship between Magdalenian subsistence and environmental change: the mammalian evidence from El Mirón (Spain). Quat. Int. 272–273, 125–137.
Dansgaard, W., Johnsen, S.J., Clausen, H.B., Dahl-Jensen, D., Gundestrup, N.S., Hammer, C.U., Hvidberg, C.S., Steffensen, J.P., Sveinbjörnsdottir, A.E., Jouzel, J., Bond, G., 1993. Evidence for general instability of past climate from a 250-kyr ice-core record. Nature 364, 218–220.
Darviche, D., Orth, A., Michaux, J., 2006. Mus spretus et M. Musculus (Rodentia, Mammalia) en zone méditerranéenne: différenciation biométrique et morphologique: application à des fossiles marocains pléistocènes. Mammalia 70 (1–2), 90–97.

deMenocal, P., Ortiz, J., Guilderson, T., Adkins, J., Sarnthein, M., Baker, L., Yarusinsky, M., 2000. Abrupt onset and termination of the African humid period: rapid climate responses to gradual insolation forcing. Quat. Sci. Rev. 19, 347–361.
deMenocal, P.B., 2001. Cultural responses to climate Change during the Late Holocene. Science 292 (5517), 667–673.
Domínguez García, Á.C., Laplana, C., Sevilla, P., Blain, H.-A., Palomares Zumajo, N., de Lugo, Benítez, Enrich, L., 2019. New data on the introduction and dispersal process of small mammals in southwestern Europe during the Holocene: Castillejo del Bonete site (southeastern Spain). Quat. Sci. Rev. 225, 106008.
Domínguez García, Á.C., Laplana, C., Sevilla, P., 2020. Early reliable evidence of the Etruscan shrew (Suncus etruscus) in southwestern Europe during ancient times. Reconstructing its dispersal process along the Mediterranean Basin. Quat. Sci. Rev. 250, 106690.
Domínguez-García, Á.C., Laplana, C., Sevilla, P., Álvarez-Vena, A., Collado Giraldo, H., 2022. Small mammals of the Holocene sequence of Postes Cave (SW Spain): biogeographic and palaeoenvironmental implications for southwestern Iberia. Hist. Biol. https://doi.org/10.1080/08912963.2022.2045981.
Doughty, C.E., Wolf, A., Field, C.B., 2010. Biophysical feedbacks between the Pleistocene megafauna extinction and climate: the first human-induced global warming? Geophys. Res. Lett. 37, L15703.
Ellis, E.C., 2011. Anthropogenic transformation of the terrestrial biosphere. Phil. Trans. R. Soc. A 369, 1010–1035.
Evans, E.M.N., Van Couvering, J.A.H., Andrews, P., 1981. Paleoecology of Miocene sites in Western Kenya. J. Hum. Evol. 10, 99–116.
Fagoaga, A., Blain, H.-A., Marquina-Blasco, R., Laplana, C., Sillero, N., Hernández, C.M., Mallol, C., Galván, B., Ruiz-Sánchez, F.J., 2019. Improving the accuracy of small vertebrate-based palaeoclimatic reconstructions derived from the Mutual Ecogeographic Range. A case study using geographic information systems and UDA-ODA discrimination methodology. Quat. Sci. Rev. 223, 105969.
Fernández-Jalvo, Y., Andrews, P., Denys, C., Sesé, C., Stoetzel, E., Marin-Monfort, D., Pesquero, D., 2016. Taphonomy for taxonomists: implications of predation in small mammal studies. Quat. Sci. Rev. 139, 138–157.
Filipović, D., Meadows, J., Dal Corso, M., et al., 2020. New AMS 14C dates track the arrival and spread of broomcorn millet cultivation and agricultural change in prehistoric Europe. Sci. Rep. 10, 13698.
García-Morato, S., Marin-Monfort, D., Bañuls-Cardona, S., Cuenca-Bescós, G., Vergès, J. M., Fernández-Jalvo, Y., 2023. Solving a 'puzzle'. The global 4.2 ka Bond Event at El Mirador cave (Sierra de Atapuerca, Burgos, Spain) and the importance of small mammal taphonomy to the interpretation of past environments and their climatic controls. The Holocene 33 (3), 296–309.
García-Ruiz, J.M., 2010. The effects of land uses on soil erosion in Spain: a review. Catena 81, 1–11.
Garrote, A., García, J., Muñoz, L., Arriola, G., Eguiguren, E., García, I., 1993. Mapa geológico del País Vasco 1:25.000 Hoja 37-III Zierbena. Ente Vasco de la Energía.
Gómez-Olivencia, A., Cubas, M., Sala, N., Pantoja, A., Garcia-Ibaibarriaga, N., Rios-Garaizar, J., Regalado, E., Libano, I., Solar, G., Arlegi, M., Moreno, J., 2015. Restos humanos calcolíticos de dos nuevos yacimientos de Punta Lucero (Zierbena, Bizkaia). Kobie Serie Paleoantropología 34, 5–18.
González Oreja, J.A., Lorenzo Rodolfo, J.C., Pérez de Ana, J.M., 1993. Nota sobre la alimentación de la lechuza común en dos zonas de Vizcaya. Estudios del Museo de Ciencias Naturales de Álava 8, 227–230.
González-Rabanal, B., Marín-Arroyo, A.B., Cristiani, E., Zupancich, A., González-Morales, M.R., 2022. The arrival of millets to the Atlantic coast of northern Iberia. Sci. Rep. 12, 18589.
Gutiérrez, J., Aleix-Mata, G., Lamelas, L., Arroyo, M., Marchal, J.A., Sánchez, A., 2019. Karyotype analysis of the new Talpa species Talpa Aquitania (Talpidae; Insectivora) from Northern Spain. Cytogenet. Genome Res. 159 (1), 26–31.
Hammer, Ø., Harper, D.A.T., Ryan, P.D., 2001. PAST: Paleontological statistics software package for education and data analysis. Palaeontol. Electron. 4 (1), 1–9.
Hillson, S., 2005. Teeth. In: Manuals in Archaeology. Cambridge University Press.
Horáček, I., Knitlová, M., Wagner, J., Kordos, L., Nadachowski, A., 2013. Late Cenozoic history of the Genus Micromys (Mammalia, Rodentia) in Central Europe. PLoS ONE 8 (5), e62498.
Iriarte, M.J., 1994. Estudio palinológico del nivel sepulcral del yacimiento arqueológico de Pico Ramos (Muskiz, Bizkaia). Cuadernos de Sección. Prehistoria-Arqueología 5, 161–179.
Iriarte, M.J., Mujika, J., Tarriño, A., 2005. Herriko Barra (Zarautz-Gipuzkoa): caractérisation industrielle et économique des premiers groupes de producteurs sur le littoral basque. In: Marchand, G., Tresset, A. (Eds.), Actas del Colloque Unité et diversité des processus de néolithisation sur la façade atlantique de l'Europe. Bulletin de la Société Préhistorique Française XXXVI, pp. 127–136.
Jalut, G., Amat, A.E., Bonnet, L., Gauquelin, T., Fontugne, M., 2000. Holocene climatic changes in the Western Mediterranean, from south-East France to south-East Spain. Palaeogeogr. Palaeoclimatol. Palaeoecol. 160 (3–4), 255–290.
Jones, J.R., Richards, M.P., Reade, H., Bernaldo de Quirós, F., Marín-Arroyo, A.B., 2019. Multi-Isotope investigations of ungulate bones and teeth from El Castillo and Covalejos caves (Cantabria, Spain): Implications for paleoenvironment reconstructions across the Middle-Upper Palaeolithic transition. J. Archaeol. Sci. Rep. 23, 1029–1042.
Jones, J.R., Marín-Arroyo, A.B., Corchón Rodríguez, M.S., Richards, M.P., 2021. After the Last Glacial Maximum in the refugium of northern Iberia: environmental shifts, demographic pressure and changing economic strategies at Las Caldas Cave (Asturias, Spain). Quat. Sci. Rev. 262, 106931.
Knitlová, M., Horáček, I., 2017. Late Pleistocene-Holocene paleobiogeography of the genus Apodemus in Central Europe. PLoS One 12 (3), e0173668.
Krajcarz, M.T., Szymanek, M., Krajcarz, M., Pereswiet-Soltan, A., Alexandrowicz, W.P., Sudoł-Procyk, M., 2020. Shelter in Smollen III - a unique example of stratified Holocene clastic cave sediments in Central Europe, a lithostratigraphic stratotype and a record of regional paleoecology. PLOS ONE 15 (2), e0228546.
Krapp, F., Niethammer, J., 1982. Microtus agrestis (Linnaeus, 1761) – Erdmaus. In: Niethammer, J., Krapp, F. (Eds.), Handbuch der Säugetiere Europas. Band 2/1. Nagetiere II. Akademische Verlagsgesellschaft, Wiesbaden, pp. 349–373.
Kryštufek, B., Shenbrot, G.I., 2022. Voles and Lemmings (Arvicolinae) of the Palaearctic Region. University Press, Maribor. https://doi.org/10.18690/um.fnm.2.2022.
Kryštufek, B., Tesakov, A.S., Lebedev, V.S., Bannikova, A.A., Abramson, N.I., Shenbrot, G., 2020. Back to the future: the proper name for red-backed voles is Clethrionomys Tilesius and not Myodes Pallas. Mammalia 84 (2), 214–217.
Laskar, J., Robutel, P., Joutel, F., Gastineau, M., Correia, A.C.M., Levrard, B., 2004. A long-term numerical solution for the insolation quantities of the Earth. Astronomy Astrophys. 428 (1), 261–285.
Lazaridis, I., Alpaslan-Roodenberg, S., Acar, A., et al., 2022. The genetic history of the Southern Arc: a bridge between West Asia and Europe. Science 377 (6609).
Liu, C., Kong, Z., Lang, S.D., 2004. Dadiwan yizhi nongye zhiwu yicun yu renlei shengcun huanjing de tantao (A discussion on agricultural and botanical remains and the human ecology of Dadiwan site). Zhongyuan Wenwu (Cultural Relics Central China) 4, 25–29.
Llorente, L., 2010. The Hares from Cova Fosca (Castellón, Spain). Archaeofauna 19, 59–97.
López-Fuster, M.J., Ventura, J., Miralles, M., Castién, E., 1990. Craniometrical characteristics of Neomys fodiens (Pennant, 1771) (Mammalia, Insectívora) from the northeastern Iberian Peninsula. Acta Theriol. 35 (3–4), 269–276.
López-García, J.M., 2008. Evolución de la diversidad taxonómica de los micromamíferos en la Península Ibérica y cambios Paleoambientales durante el Pleistoceno Superior. Unpublished Ph.D. Universitat Rovira i Virgili, Tarragona.
López-García, J.M., Blain, H.-A., Cuenca-Bescós, G., Alonso, C., Alonso, S., Vaquero, M., 2011. Small vertebrates (Amphibia, Squamata, Mammalia) from the late Pleistocene-Holocene of the Valdavara-1 cave (Galicia, northwestern Spain). Geobios 44, 253–269.
López-García, J.M., Blain, H.-A., Morales, J.I., Lorenzo, C., Bañuls-Cardona, S., Cuenca-Bescós, G., 2013. Small-mammal diversity in Spain during the late Pleistocene to early Holocene: climate, landscape, and human impact. Geology 41 (2), 267–270.
López-García, J.M., Berto, C., Colamussi, V., Dalla Valle, C., Lo Vetro, D., Luzi, E., Malavasi, G., Martini, F., Sala, B., 2014. Palaeoenvironmental and palaeoclimatic reconstruction of the lastest Pleistocene-Holocene sequence from Grotta del Romito (Calabria, southern Italy) using the small-mammal assemblages. Palaeogeogr. Palaeoclimatol. Palaeoecol. 409, 169–179.
López Merino, L., 2009. Paleoambiente y antropización en Asturias durante el Holoceno. PhD Thesis. Universidad Autónoma de Madrid. Departamento de Ecología, Madrid.
López-Merino, L., Martínez-Cortizas, A., López-Sáez, J.A., 2010. Early agriculture and palaeoenvironmental history in the North of the Iberian Peninsula: a multi-proxy analysis of the Monte Areo mire (Asturias, Spain). J. Archaeol. Sci. 37, 1978–1988.
Luzi, E., López-García, J.M., 2019. Patterns of variation in Microtus arvalis and Microtus agrestis populations from Middle to late Pleistocene in southwestern Europe. Hist. Biol. 31 (5), 535–543.
Lyman, R.L., 1984. Bone density and differential survivorship of fossil classes. J. Anthropol. Archaeol. 3, 259–299.
Mallye, J.-B., Cochard, D., Laroulandie, V., 2008. Accumulations osseuses en périphérie de terriers de petits carnivores : les stigmates de prédation et de fréquentation. Annales Paléontol. 94 (3), 187–208.
Mariezkurrena, K., 1983. Contribución al conocimiento del desarrollo de la dentición y el esqueleto postcraneal de Cervus elaphus. Munibe (Antropologia-Arkeologia) 35, 149–202.
Mariezkurrena, K., 1990. Caza y Domesticación durante el Neolítico y Edad de los Metales en el País Vasco. Munibe (Antropologia-Arkeologia) 42, 241–252.
Marín-Arroyo, A.B., 2010. Arqueozoología en el cantábrico oriental durante la transición Pleistoceno/Holoceno. La cueva del Mirón, PubliCan, Ediciones de la Universidad de Cantabria, Santander.
Martín-Chivelet, J., Muñoz-García, M.B., Edwards, R.L., Turrero, M.J., Ortega, A.I., 2011. Land surface temperature changes in Northern Iberia since 4000 yr BP, based on δ13C of speleothems. Glob. Planet. Change 77 (1–2), 1–12.
Martínez-Solano, I., Sanchiz, B., 2005. Anfibios y Reptiles del Pleistoceno medio de Ambrona. Zona Arqueológica 5, 232–239.
Martínez-Villa, A., Álvarez-Fernández, E., Álvarez-Vena, A., Arrojo, L., Ballesteros, D., Cubas, M., Drak, L., Llorente Rodríguez, L., Martín-Jarque, S., Gil, M., 2022. New insights into upper Palaeolithic and Mesolithic occupations in Les Pedroses cave (Asturies, North Spain). J. Archaeol. Sci. Rep. 45, 103592.
Mayewski, P.A., Rohling, E.E., Stager, J.C., Karlén, W., Maasch, K.A., Meeker, L.D., Meyerson, E.A., Gasse, F., van Kreveld, S., Holmgren, K., Lee-Thorp, J., Rosqvist, G., Rack, F., Staubwasser, M., Schneider, R.R., Steig, E.J., 2004. Holocene climate variability. Quat. Res. 62 (3), 243–255.
Miller, G.H., Geirsdottir, A., Zhong, Y., Larsen, D., Otto-Bliesner, B.L., Holland, M.M., Bailey, D.A., Refsnider, K.A., Lehman, S.J., Southon, J.R., Anderson, C., Björnsson, H., Thordarson, T., 2012. Abrupt onset of the Little Ice Age triggered by volcanism and sustained by sea-ice/ocean feedbacks. Geophys. Res. Lett. 39, L02708.
Miller, N.F., Spengler, R.N., Frachetti, M., 2016. Millet cultivation across Eurasia: origins, spread, and the influence of seasonal climate. The Holocene 26 (10), 1566–1575.
Mistrot, V., 2011. Les micromammifères du site gallo-romain de Melun-Grüber (Seine-et-Marne). Bulletin de l'Association des Naturalistes de la Vallée du Loing 87 (3), 132–141.

Mistrot, V., 2013. Les micromammifères des couches 37 à 33 de la grotte du Gardon: une emprise agricole naissante?. In: Perrin T., Voruz J.-L. (dir.) La grotte du Gardon (Ain) Volume II. Du Néolithique moyen II au Bronze ancien (couches 46 à 33), pp. 353–356.
Mistrot, V., 2013. Les micromammifères des couches 47 à 39 de la grotte du Gardon: une anthropisation du milieu très limitée.. In: Perrin T., Voruz J.-L. (dir.) La grotte du Gardon (Ain) Volume II. Du Néolithique moyen II au Bronze ancien (couches 46 à 33), pp. 229–232.
Moclán, A., Domínguez-García, A.C., Stoetzel, E., Cucchi, T., Sevilla, P., Laplana, C., 2023. Machine Learning interspecific identification of mouse first lower molars (genus Mus Linnaeus, 1758) and application to fossil remains from the Estrecho Cave (Spain). Quat. Sci. Rev. 299, 107877.
Muñoz Sobrino, C., Ramil-Rego, P., Gómez-Orellana, L., Díaz Varela, R.A., 2005. Palynological data on major Holocene climatic events in NW Iberia. Boreas 34, 381–400.
Nadachowski, A., 1984. Taxonomic value of anteroconid measurements of M1 in common and field voles. Acta Theriol. 29 (10), 123–143.
Nicolas, V., Martínez-Vargas, J., Hugot, J.-P., 2015. *Talpa aquitania* nov. sp. (Talpidae, Soricomorpha) a new mole species from Southwest France and North Spain. Bulletin de l'Académie Vétérinaire de France 168 (4), 329–334.
Nicolas, V., Martínez-Vargas, J., Hugot, J.-P., 2017. *Talpa aquitania* sp. nov. (Talpidae, Soricomorpha), a new mole species from SW France and N Spain. Mammalia 81 (6), 641–642.
Niethammer, J., 1990. Talpa. In: Niethammer, J., Krapp, F. (Eds.), Handbuch der Säugetiere Europas. Band 3/1. Insektenfresser-Insectivora, Herrentiere-Primates. Aula-Verlag, Wiesbaden, pp. 93–161.
Noddle, B., 1974. Ages of epiphyseal closure in feral and domestic goats and ages of dental eruption. J. Archaeol. Sci. 1 (2), 195–204.
Nores, C., 1988. Diferenciación biométrica de Apodemus sylvaticus y Apodemus flavicollis en la Cordillera Cantábrica. Primeros resultados. Revista de Biología de la Universidad de Oviedo 6, 109–116.
Nores, C., 1989. Variación temporal y espacial de micromamíferos: determinación mediante análisis de egagrópilas de Tyto alba. Ph.D. Thesis. Departamento de Biología de Organismos y Sistemas, Facultad de Biología, Universidad de Oviedo.
Nores, C., Sánchez-Canals, J.L., Castro, A., González, G.R., 1982. Variation du genre Neomys Kaup, 1829 (Mammalia, Insectívora) dans le secteur cantabro-galicien de la péninsule Ibérique. Mammalia 46, 361–373.
Olalde, I., Mallick, S., Patterson, N., et al., 2019. The genomic history of the Iberian Peninsula over the past 8000 years. Science 363 (6432), 1230–1234.
Ordiales, A., Suárez-Bilbao, A., Garcia-Ibaibarriaga, N., Ibarra, J.L., Murelaga, X., 2015. Estudio de los micromamíferos de los lechos de la Edad del Bronce de la Cueva de Arenaza I (Galdames, Bizkaia). Geogaceta 58, 51–54.
Palacios, F., López Martínez, N., 1980. Morfología dentaria de las liebres europeas (Lagomorpha, Leporidae). Doñana Acta Vertebrata 7 (1), 61–81.
Pales, L., Lambert, C., 1971. Atlas Osteologique Pour Servir à l'identificátion Des Mammiféres du Quaternaire. Editions du Centre National de la Recherche Scientifique, Paris.
Palomo, L.J., Gisbert, J., Blanco, J.C., 2007. Atlas Y Libro Rojo de los Mamíferos Terrestres de España. Dirección General para la Biodiversidad-SECEM-SECEMU, Madrid, Spain.
Pasquier, L., 1974. Dynamique évolutive d'un sous-genre de Muridae, Apodemus (Sylvaemus). Etude biometrique des caractères dentaires des populations fossiles et actuelles d'Europe Occidentale. Thèse. Université des Sciences et Techniques du Lanquedoc, Montpellier.
Patino, S., Valencia, J., Elorza, J., Prieto, A., 2002. La flora del monte Serantes. Bizkaiko Gaiak / Temas Vizcaínos 331–332, 183 pp.
Patterson, N., Isakov, M., Booth, T., et al., 2022. Large-scale migration into Britain during the Middle to Late Bronze Age. Nature 601, 588–594.
Paupério, J., Herman, J.S., Melo-Ferreira, J., Jaarola, M., Alves, P.C., Searle, J.B., 2012. Cryptic speciation in the field vole: a multilocus approach confirms three highly divergent lineages in Eurasia. Mol. Ecol. 21, 6015–6032.
Pelletier, M., 2018. Évolution morphométrique et Biogéographie des Léporidés dans les environnements méditerranéens au Pléistocène. Implications socio-économiques pour les sociétés humaines. Thése. Aix-Marseille Université.
Pemán, E., 1983. Biometría y sistemática del género Neomys Kamp 1771 (Mammalia, Insectivora) en el País Vasco. Munibe 35 (1–2), 115–148.
Pemán, E., 1990. Los micromamíferos de la cueva de Amalda y su significado. Comentarios sobre Pliomys lenki (Heller, 1930) (Rodentia, Mammalia). In: La cueva de Amalda (Zestoa, País Vasco): ocupaciones paleolíticas y postpaleolíticas. Colección Barandiaran (4). Eusko Ikaskuntza, pp. 225–238.
Peña-Chocarro, L., Zapata, L., Iriarte, M.J., González-Morales, M.R., Straus, L.G., 2005. The oldest agriculture in northern Atlantic Spain: new evidence from El Mirón Cave (Ramales de la Victoria, Cantabria). J. Archaeol. Sci. 32 (4), 579–587.
Pérez-Díaz, S., López-Sáez, J.A., Pontevedra-Pombal, X., Souto-Souto, M., Galop, D., 2016. 8000 years of vegetation history in the northern Iberian Peninsula inferred from the palaeoenvironmental study of the Zalama ombrotrophic bog (Basque-Cantabrian Mountains, Spain). Boreas 45 (4), 658–672.
Pérez-Díaz, S., López-Sáez, J.A., Núñez de la Fuente, S., Ruiz-Alonso, M., 2018. Early farmers, megalithic builders and the shaping of the cultural landscapes during the Holocene in Northern Iberian mountains. A palaeoenvironmental perspective. J. Archaeol. Sci. Rep. 18, 463–474.
Pérez-Obiol, R., García-Codron, J.C., Pèlachs, A., Pérez-Haase, A., Soriano, J.M., 2016. Landscape dynamics and fire activity since 6740 cal yr BP in the Cantabrian region (La Molina peat bog, Puente Viesgo, Spain). Quat. Sci. Rev. 135, 65–78.
Ramil-Rego, P., Rodríguez-Guitián, M., Muñoz-Sobrino, C., 1998. Sclerophyllous vegetation dynamics in the north of the Iberian peninsula during the last 16,000 years. Glob. Ecol. Biogeogr. Lett. 7, 335–351.
Reimer, P.J., Austin, W.E.N., Bard, E., et al., 2020. The IntCal20 Northern Hemisphere Radiocarbon Age Calibration Curve (0–55 cal kBP). Radiocarbon 62 (4), 725–757.
Román, J., 2019. Manual para la identificación de los cráneos de los roedores de la península ibérica, islas baleares y canarias. Manuales de Mastozoología de la SECEM.
Rosengren, E., Acatrinei, A., Cruceru, N., Dehasque, M., Haliuc, A., Lord, E., Mircea, C.I., Rusu, I., Mármol-Sánchez, E., Kelemen, B.S., Meleg, I.N., 2021. Ancient. Diversity 13 (8), 370.
Royer, A., Laroulandie, V., Bailon, S., Boudadi-Maligne, M., Costamagno, S., Danger, M., Mallye, J.-B., Rofes, J., 2021. Des restes de faune aux paléoenvironnements de Peyzaret. Estudios 43, 35–48.
Ruddiman, W.F., Thomson, J.S., 2001. The case for human causes of increased atmospheric CH4 over the last 5000 years. Quat. Sci. Rev. 20, 1769–1777.
Ruprecht, A.J., 1971. Taxonomic value of mandible measurements in Soricidae (Insectívora). Acta Theriol. 16 (21), 341–357.
Sánchez, A., 1983. Estudio comparativo de las faunas pleistocénicas y actuales de micromamíferos (Insectívoros y Roedores) en Puenteviesgo (Santander). Unpublished bachelor's thesis. Facultad de Biología, UCM in press.
Schmid, E., 1972. Atlas of Animal Bones. Elsevier Publishing Company, London.
Serjeantson, D., 2011. In: Review of animal remains from the Neolithic and early Bronze age of southern Britain (4000 BC–1500 BC).Research Department Report Series, pp. 1–170.
Sigl, M., Winstrup, M., McConnell, J., et al., 2015. Timing and climate forcing of volcanic eruptions for the past 2,500 years. Nature 523, 543–549.
Silver, I.A., 1980. La determinación de la edad en los animales domésticos. In: Brothwell, D.R., Higgs, E. (Eds.), Ciencia en Arqueología, Madrid, Fondo de Cultura Económica, pp. 290–307.
Steinhilber, F., Abreu, J.A., Beer, J., Brunner, I., Christl, M., Fischer, H., Heikkilä, U., Kubik, P.W., Mann, M.E., McCracken, K.G., Miller, H., Miyahara, H., Oerter, H., Wilhelms, F., 2012. 9,400 years of cosmic radiation and solar activity from ice cores and tree rings. Proc. Nat. Acad. Sci. 109 (16), 5967–5971.
Steinhilber, F., Beer, J., Fröhlich, C., 2009. Total solar irradiance during the Holocene. Geophys. Res. Lett. 36 (19), L19704.
Tomé, C., Vigne, J.D., 2003. Roe deer (Capreolus capreolus) age at death estimates: new methods and modern reference data for tooth eruption and wear, and for epiphyseal fusion. Archaeofauna 12, 157–173.
Valenzuela-Lamas, S., Baylac, M., Cucchi, T., Vigne, J.-D., 2011. House mouse dispersal in Iron Age Spain: a geometric morphometrics appraisal. Biol. J. Linn. Soc. 102 (3), 483–497.
Van Geel, B., Buurman, J., Waterbolk, H.T., 1996. Archaeological and palaeoecological indications of an abrupt climate change in the Netherlands, and evidence for climatological teleconnections around 2650 BP. J. Quat. Sci. 11 (6), 451–460.
Vega-Maeso, C., Carmona-Ballestero, E., Sierra Sainz-Aja, A., Marín-Arroyo, A.B., 2016. El Abrigo de la Castañera (Cantabria, Spain): a Chalcolithic cattle stable? Quat. Int. 414, 226–235.
Villalba-Mouco, V., Oliart, C., Rihuete-Herrada, C., et al., 2021. Genomic transformation and social organization during the Copper Age-Bronze Age transition in southern Iberia. Sci.Adv. 7 (47), eabi7038.
Vitousek, P.M., Mooney, H.A., Lubchenco, J., Melillo, J.M., 1997. Human domination of earth's ecosystems. Science 277, 494–499.
Walker, M., Head, M.J., Berkelhammer, M., Björck, S., Cheng, H., Cwynar, L., Fisher, D., Gkinis, V., Long, A., Lowe, J., Newnham, R., Rasmussen, S.O., Weiss, H., 2018. Formal ratification of the subdivision of the Holocene Series/Epoch (Quaternary System/Period): two new Global Boundary Stratotype Sections and Points (GSSPs) and three new stages/subseries. Episodes 41, 213–223.
Wanner, H., Beer, J., Bütikofer, J., Crowley, T.J., Cubasch, U., Flückiger, J., Goosse, H., Grosjean, M., Joos, F., Kaplan, J.O., Küttel, M., Müller, S.A., Prentice, I.C., Solomina, O., Stocker, T.F., Tarasov, P., Wagner, M., Widmann, M., 2008. Mid- to late Holocene climate change: an overview. Quat. Sci. Rev. 27 (19–20), 1791–1828.
Wilkin, S., Ventresca Miller, A., Fernandes, R., et al., 2021. Dairying enabled early Bronze Age Yamnaya steppe expansions. Nature 598, 629–633.
Wilson, D.E., Lacher, T.E., Mittermeier, R.A., 2016. Handbook of the Mammals of the World: 6. Lagomorphs and Rodents I. Lynx Edicions, Barcelona, Spain.
Wilson, D.E., Lacher, T.E., Mittermeier, R.A., 2017. Handbook of the Mammals of the World: 7. Rodents II. Lynx Edicions, Barcelona, Spain.
Wilson, D.E., Mittermeier, R.A., 2018. Handbook of the Mammals of the World: 8. Insectivores, Sloths and Colugos. Lynx Edicions, Barcelona, Spain.
Yasuda, S.P., Vogel, P., Tsuchiya, K., Han, S.-H., Lin, L.-K., Suzuki, H., 2005. Phylogeographic patterning of mtDNA in the widely distributed harvest mouse (Micromys minutus) suggests dramatic cycles of range contraction and expansion during the mid- to late Pleistocene. Can. J. Zool. 83 (11), 1411–1420.
Zapata, L., 1995. The excavation of the burial cave Pico Ramos (Muskiz, Biscay). The ornamental and bone industry. In: Zapata, L. (Ed.), The Chalcolithic burial deposit of the cave Pico Ramos (Muskiz, Biskay). Munibe (Antropologia-Arkeologia) 47, pp. 35–90.
Zapata Peña, L., 1999. El combustible y la agricultura prehistórica. Estudio arqueobotánico de los yacimientos de Arenaza, Kanpanoste Goikoa y Kobaederra (Fuelwood and prehistoric agriculture. Archaeobotanical analyses from the cave sites Arenaza, Kanpanoste Goikoa and Kobaederra). Isturitz 10, 305–337.
Zapata Peña, L., 2002. Origen de la agricultura en el País Vasco y transformaciones en el paisaje: análisis de restos vegetales arqueológicos. Kobie 4, 223 p.
Zapata Peña, L., Peña-Chocarro, L., Pérez Jordá, G., Stika, H.-P., 2005. Difusión de la agricultura en la Península Ibérica. In: Arias, P., Ontañón, R., García-Moncó, C. (Eds.), III Congreso del Neolítico en la Península Ibérica, pp. 103–113.